

Accounting for multiple imputation-induced variability for differential analysis in mass spectrometry-based label-free quantitative proteomics

Marie Chion^{1,2*}, Christine Carapito² and Frédéric Bertrand^{1,3}

¹Institut de Recherche Mathématique Avancée, UMR 7501, 7 rue René Descartes, 67084 Strasbourg Cedex, France.

²Laboratoire de Spectrométrie de Masse Bio-Organique, Institut Pluridisciplinaire Hubert Curien, UMR 7178, 25 rue Becquerel, 67087 Strasbourg Cedex, France.

³Laboratoire de Modélisation et Sécurité des Systèmes, Institut Charles Delaunay, UMR CNRS 6281, Université de Technologie de Troyes, 12 Rue Marie Curie, 42060 Troyes Cedex, France.

* **Contact:** marie.chion@protonmail.com

Abstract

Motivation: Imputing missing values is common practice in label-free quantitative proteomics. Imputation aims at replacing a missing value with a user-defined one. However, the imputation itself may not be optimally considered downstream of the imputation process, as imputed datasets are often considered as if they had always been complete. Hence, the uncertainty due to the imputation is not adequately taken into account. We provide a rigorous multiple imputation strategy, leading to a less biased estimation of the parameters' variability thanks to Rubin's rules. The imputation-based peptide's intensities' variance estimator is then moderated using Bayesian hierarchical models. This estimator is finally included in moderated t -test statistics to provide differential analyses results. This workflow can be used both at peptide and protein-level in quantification datasets. For protein-level results based on peptide-level quantification data, an aggregation step is also included.

Results: Our methodology, named **mi4p**, was compared to the state-of-the-art **limma** workflow implemented in the **DAPAR** R package, both on simulated and real datasets. We observed a trade-off between sensitivity and specificity, while the overall performance of **mi4p** outperforms **DAPAR** in terms of F -Score.

Availability: The methodology here described is implemented under the R environment and can be found on GitHub: <https://github.com/mariechion/mi4p>. The R scripts which led to the results presented here can also be found on

this repository. The real datasets are available on ProteomeXchange under the dataset identifiers PXD003841 and PXD027800.

1 Introduction

Dealing with incomplete data is one of the main challenges as far as statistical analysis is concerned. Different strategies can be used to tackle this issue. The simplest way consists of deleting from the dataset the observations for which there are too many missing values, leading to a complete-case dataset. However, it causes information loss, might create bias and could ultimately result in poorly informative datasets.

Another way to cope with missing data is to use methods that account for the missing information. For the last decades, researchers advocated the use of a single technique called imputation. Imputing missing values consists of replacing a missing value with a value derived using a user-defined formula (such as the mean, the median or a value provided by an expert, thus considering the user’s knowledge). Hence it makes it possible to perform the analysis as if the data were complete. More particularly, the vector of parameters of interest can be then estimated.

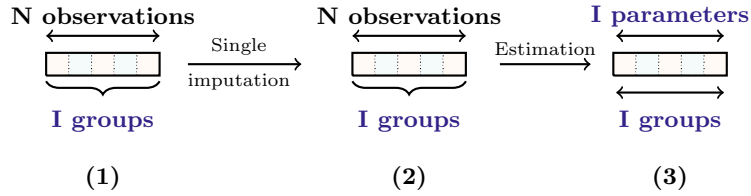


Figure 1: **Single imputation.** (1) Initial dataset with missing values. It is supposed to be made of N observations that are split into I groups. (2) Single imputation provides an imputed dataset. (3) The vector of parameters of interest is estimated based on the single imputed dataset.

Single imputation means completing the dataset once and considering the imputed dataset as if it was never incomplete, see Figure 1. However, single imputation has the major disadvantage of discarding the variability from the missing data and the imputation process. It may also lead to a biased estimator of the vector of parameters of interest.

Multiple imputation described by Little and Rubin (2019) closes this loop-hole by generating several imputed datasets. These datasets are then used to build a combined estimator of the vector of parameters of interest, by usually using the mean of the estimates among all the imputed datasets, see Figure 2. This combined estimator is known as the first Rubin’s rule. The second Rubin’s rule states a formula to estimate the variance of the combined estimator, decomposing it as the sum of the intra-imputation variance component and the between-imputation component. The rule of thumb suggested by White *et al.*

(2011) takes the number of imputed datasets as the percentage of missing values in the original dataset. Recent work focused on better estimating the Fraction of Missing Information (Pan, Q. *et al.*) or improving that rule (von Hippel, P. T.). Note that Rubin’s rules cannot be used in order to get a combined imputed dataset but instead provide an estimator of the vector of parameters of interest and an estimator of its covariance matrix both based on multiple imputation, see Figure 2.

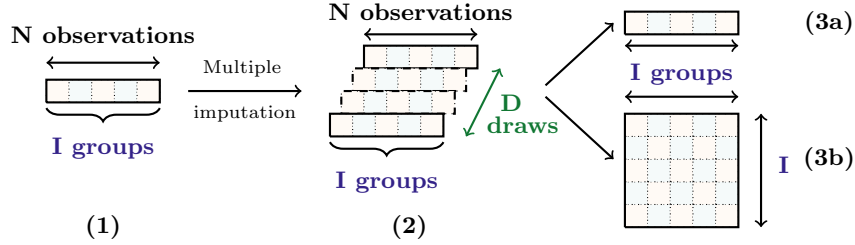


Figure 2: **Multiple imputation strategy.** (1) Initial dataset with missing values. It is supposed to have N observations that are split into I groups. (2) Multiple imputation provides D estimators for the vector of parameters of interest. (3a) The D estimators are combined using the first Rubin’s rule to get the combined estimator. (3b) The estimator of the variance-covariance matrix of the combined estimator is provided by the second Rubin’s rule.

Dealing with missing values is also one of the main struggles in label-free quantitative proteomics. Intensities of thousands of peptides are obtained by liquid chromatography-tandem mass spectrometry, using extracted ion chromatograms. Several reasons may cause missing peptides’ intensities. Either the considered peptide is missing in the given biological sample, and the intensity is then missing not at random (MNAR), or it was missed during the acquisition process and, the intensity is then missing at random (MAR).

In state-of-the-art software for statistical analysis in label-free quantitative proteomics, single imputation is the most commonly used method to deal with missing values. In the **MSstats** R package (available on Bioconductor), Choi *et al.* (2014) distinguish missing completely at random values and missing values due to low intensities. The user can then choose to impute the censored value using a threshold value or an Accelerated Failure Time model. The Perseus software by Tyanova *et al.* (2016) offers three methods for single imputation: either imputing by "NaN", impute by a user-defined constant or impute according to a Gaussian distribution in order to simulate intensities, which are lower than the limit of detection. Recently, Goeminne *et al.* (2020) implemented a single imputation method based on a hurdle model in their **MSqRob** R package (Goeminne *et al.*, 2018). As far as machine learning is concerned, Song and Yu (2021) suggested a method for imputing missing values in label-free mass spectrometry-based proteomics datasets, called **XGboost**.

The ProStaR software based on the **DAPAR** R package and developed by Wic-

zorek *et al.* (2017) splits missing values into two categories, whether they are Missing in an Entire Condition (MEC) or Partially Observed Values (POV) (Lazar *et al.*, 2016). The software allows single imputation, using either a small quantile from the distribution of the considered biological sample, the k -Nearest Neighbours (kNN) algorithm or the Structured Least Squares Adaptative algorithm or by choosing a fixed value. The PANDA-view software developed by Chang *et al.* (2018) also enables the use of the kNN algorithm or a fixed value. Moreover, both software programs give the possibility to impute the dataset several times before combining the imputed datasets in order to get a final dataset without any missing values. PANDA-view relies on the `mice` R package by Van Buuren and Groothuis-Oudshoorn, (2011), whereas ProStaR accounts for the nature of missing values and imputes them with the `imp4p` R package implemented by Gai Gianetto *et al.* (2020). However, both software programs consider the final dataset as if it had always been complete. The uncertainty due to multiple imputation is not properly taken into account downstream of the imputation step.

In the following, we will conduct the multiple imputation process to its end, as described by Little and Rubin (2019) and use the imputed datasets to provide a combined estimator of the vector of parameters of interest as well as a combined estimator of its variance-covariance matrix estimator. We will then project this matrix to get a unidimensional variance estimator before moderating it using the empirical Bayes procedure defined in the seminal paper of Smyth *et al.* (2004) and later developed by Phipson *et al.* (2016). It is well known that such a moderating step highly improves the following statistical analyses such as significance testing of confidence interval estimation, both at the peptide level (Suomi *et al.*, 2015; Goeminne *et al.*, 2015) or the protein level (Goeminne *et al.*, 2015, 2016).

2 Materials

2.1 Simulated datasets

We evaluated our methodology on three types of simulated datasets. First, we considered an experimental design where the distributions of the two groups to be compared scarcely overlap. This design led to a fixed effect one-way analysis of variance model (ANOVA), which can be written as:

$$y_{ij} = \mu + \delta_{ij} + \epsilon_{ij} \quad (1)$$

with $\mu = 100$, $\delta_{ij} = 100$ if $1 \leq i \leq 10$ and $j = 2$ and $\delta_{ij} = 0$ otherwise and $\epsilon_{ijk} \sim \mathcal{N}(0, 1)$. Here, y_{ij} represents the log-transformed abundance of peptide i in the j -th sample. Thus, we generated 100 datasets by considering 200 individuals and 10 variables, divided into 2 groups of 5 variables, using the following steps:

1. For the first 10 rows of the data frame, set as differentially expressed, draw the first 5 observations (first group) from a Gaussian distribution with a

mean of 100 and a standard deviation of 1. Then draw the remaining 5 observations (second group) from a Gaussian distribution with a mean of 200 and a standard deviation of 1.

2. For the remaining 190 rows, set as non-differentially expressed, draw the first 5 observations as well as the last 5 observations from a Gaussian distribution with a mean of 100 and a standard deviation of 1.

Secondly, we considered an experimental design, where the distributions of the two groups to be compared might highly overlap. Hence, we based it on the random hierarchical ANOVA model by Lazar *et al.* (2016), derived from Karpievitch *et al.* (2012). The simulation design follows the following model:

$$y_{ij} = P_i + G_{ik} + \epsilon_{ij\mathbf{k}} \quad (2)$$

where y_{ij} is the log-transformed abundance of peptide i in the j -th sample, P_i is the mean value of peptide i , G_{ik} is the mean differences between the condition groups, and ϵ_{ij} is the random error terms, which stands for the peptide-wise variance. We generated 100 datasets by considering 1000 individuals and 20 variables, divided into 2 groups of 10 variables, using the following steps:

1. Generate the peptide-wise effect P_i by drawing 1000 observations from a Gaussian distribution with a mean of 1.5 and a standard deviation of 0.5.
2. Generate the group effect G_{ik} by drawing 200 observations (for the 200 individuals set as differentially expressed) from a Gaussian distribution with a mean of 1.5 and a standard deviation of 0.5 and 800 observations fixed to 0.
3. Build the first group dataset by replicating 10 times the sum of P_i and the random error term, drawn from a Gaussian distribution of mean 0 and standard deviation 0.5.
4. Build the second group dataset by replicating 10 times the sum of P_i , G_{ik} and the random error term drawn from a Gaussian distribution of mean 0 and standard deviation 0.5.
5. Bind both datasets to get the complete dataset.

Finally, we considered an experimental design similar to the second one, but with random effects P_i and G_{ik} . The 100 datasets were generated as follows.

1. For the first group, replicate 10 times (for the 10 variables in this group) a draw from a mixture of 2 Gaussian distributions. The first one has the following parameters: a mean of 1.5 and a standard deviation of 0.5 (corresponds to P_i). The second one has the following parameters: a mean of 0 and a standard deviation of 0.5 (corresponds to ϵ_{ij}).
2. For the second group replicate 10 times (for the 10 variables in this group) a draw from a mixture of the following 3 distributions.

- (a) The first one is a Gaussian distribution with the following parameters: a mean of 1.5 and a standard deviation of 0.5 (corresponds to P_i).
- (b) The second one is the mixture of a Gaussian distribution with a mean of 1.5 and a standard deviation of 0.5 for the 200 first rows (set as differentially expressed) and a zero vector for the remaining 800 rows (set as not differentially expressed). This mixture illustrates the G_{ik} term in the previous model.
- (c) The third distribution has the following parameters: a mean of 0 and a standard deviation of 0.5 (corresponds to ϵ_{ij}).

All simulated datasets were then amputated to produce MCAR missing values in the following proportions: 1%, 5%, 10%, 15%, 20% and 25%.

2.2 Real datasets

We challenged our methodology on several real datasets coming from two different experiments described hereafter.

We consider a first real dataset from Muller *et al.* (2016). The experiment involved six peptide mixtures, composed of a constant yeast (*Saccharomyces cerevisiae*) background, into which increasing amounts of UPS1 standard proteins mixtures (Sigma) were spiked at 0.5, 1, 2.5, 5, 10 and 25 fmol, respectively. In a second well-calibrated dataset, yeast was replaced by a more complex total lysate of *Arabidopsis thaliana* in which UPS1 was spiked in 7 different amounts, namely 0.05, 0.25, 0.5, 1.25, 2.5, 5 and 10 fmol. For each mixture, technical triplicates were constituted. The *Saccharomyces cerevisiae* dataset was acquired on a nanoLC-MS/MS coupling composed of nanoAcquity UPLC device (Waters) coupled to a Q-Exactive Plus mass spectrometer (Thermo Scientific, Bremen, Germany) as extensively described in Muller *et al.* (2016). The *Arabidopsis thaliana* dataset was acquired on a nanoLC-MS/MS coupling composed of nanoAcquity UPLC device (Waters) coupled to a Q-Exactive HF-X mass spectrometer (Thermo Scientific, Bremen, Germany) as described in Supplementary data, Section S7.3.

For the *Saccharomyces cerevisiae* and *Arabidopsis thaliana* datasets, Maxquant software was used to identify peptides and derive extracted ion chromatograms. Peaks were assigned with the Andromeda search engine with full trypsin specificity. The database used for the searches was concatenated in-house with the *Saccharomyces cerevisiae* entries extracted from the UniProtKB-SwissProt database (16 April 2015, 7806 entries) or the *Arabidopsis thaliana* entries (09 April 2019, 15 818 entries) and those of the UPS1 proteins (48 entries). The maximum false discovery rate was 1% at peptide and protein levels using a target-decoy strategy. For the *Arabidopsis thaliana* + UPS1 experiment, data were extracted both with and without Match Between Runs and 2 pre-filtering criteria were applied before statistical analysis: only peptides with, on the one hand, at least 1 out of 3 quantified values in each condition and, on the other hand at least 2 out of 3, were kept. Thus, 4 datasets derived from the *Arabidopsis thaliana* + UPS1 were considered. The same filtering criteria were

applied for the *Saccharomyces cerevisiae* + UPS1 experiment, but only on data extracted with Match Between Runs, leading to 2 datasets being considered.

3 Methods

3.1 Normalization

Normalising peptides’ or proteins’ intensities aims at reducing batch effects, sample-level variations and therefore better comparing intensities across studied biological samples Wang *et al.* (2021). In this work, quantile normalisation (as described by Bolstad *et al.* (2003)) was performed using the `normalize.quantiles` function from the `preprocessCore` R package (Bolstad *et al.*, 2021).

3.2 Multiple imputation methods

Several methods for imputing missing values in mass spectrometry-based proteomics datasets were developed in the last decade. However, the recent benchmarks of imputation algorithms do not reach a consensus (as shown in Supplementary data, Table S1.1). This is mainly due to the complex nature of the underlying missing values mechanism. In this work, we chose to focus on some of the most commonly used methods 1.

Method	Implementation	References
k Nearest Neighbours	impute.knn (impute R package)	Hastie et al. (2021) Hastie et al. (1999) Troyanskaya et al. (2001)
Maximum Likelihood Estimation	impute.mle (imp4p R package)	Giai-Gianetto (2020) Schafer (1997) Van Buuren (2011)
Bayesian Linear Regression	mice (mice R package)	Van Buuren (2021) Rubin (1987) Schafer (1997)
Principal Component Analysis	impute.pca (imp4p R package)	Giai-Gianetto (2020) Josse & Husson (2013)
Random Forests	impute.RF (imp4p R package)	Giai-Gianetto (2020) Stekhoven & Buehlmann (2012)

Table 1: Overview of the imputation methods used in the evaluation of the `mi4p` workflow.

The k -Nearest Neighbours method imputes missing values by averaging the k -nearest observations of the given missing value in terms of Euclidean distance. This method was described by Hastie *et al.* (1999) and Troyanskaya *et al.* (2001)

and implemented in Hastie *et al.* (2021). The Maximum Likelihood Estimation method imputed missing values using the EM algorithm proposed by Schafer (1997) and implemented by Gai Gianetto *et al.* (2020). The Bayesian linear regression method imputes missing values using the normal model and following the method described by Rubin (1987) and implemented by Van Buuren and Groothuis-Oudshoorn, (2011). The Principal Component Analysis imputes missing values using the algorithm proposed by Josse and Husson (2013) and implemented by Gai Gianetto *et al.* (2020). The Random Forests method imputes missing values using the algorithm proposed by Stekhoven and Bühlmann (2012) and implemented by Gai Gianetto *et al.* (2020).

3.3 Estimation

The objective of multiple imputation is to estimate from D drawn datasets the vector of parameters of interest and its variance-covariance matrix. Notably, accounting for multiple-imputation-based variability is possible thanks to Rubin’s rules, which provide an accurate estimation of these parameters.

Let us consider a D -time imputed dataset with P individuals (corresponding to P peptides or proteins) and N observations (corresponding to N biological samples), divided between I groups (corresponding to I conditions to be compared). Let β_P be the vector of parameters of interest, such as :

$$\beta_P = (\beta_{P,1}, \dots, \beta_{P,I}) \quad (3)$$

The first Rubin’s rule provides the combined estimator of β_P :

$$\hat{\beta}_P = \frac{1}{D} \sum_d^D \hat{\beta}_{p,d} \quad (4)$$

where $\hat{\beta}_{p,d}$ is the estimator of β_P in the d -imputed dataset.

The second Rubin’s rule gives the combined estimator of the variance-covariance matrix for each estimated vector of parameters of interest for peptide p through the D imputed datasets such as:

$$\hat{\Sigma}_P = \frac{1}{D} \sum_{d=1}^D W_d + \frac{D+1}{D(D-1)} \sum_{d=1}^D (\hat{\beta}_{p,d} - \hat{\beta}_P)^T (\hat{\beta}_{p,d} - \hat{\beta}_P) \quad (5)$$

where W_d denotes the variance-covariance matrix of $\hat{\beta}_{p,d}$, *i.e.* the variability of the vector of parameters of interest as estimated in the d -th imputed dataset.

3.4 Projection

State-of-the-art tests, including Student’s t -test, Welch’s t -test and moderated t -test, rely on the variance estimation. Here, the variability induced by multiple imputation is described by a variance-covariance matrix. Therefore, a projection

step is required to get a unidimensional variance parameter. In our work, we chose to perform projection using the following formula :

$$\hat{s}_p = \max_k \left(\hat{\Sigma}_{p,(k,k)} \mathbf{X}^t \mathbf{X} \right) \quad (6)$$

where $\hat{\Sigma}_{p,(k,k)}$ is the k -th diagonal element of the matrix $\hat{\Sigma}_p$ and \mathbf{X} is the design matrix.

3.5 Testing

In our work, we focus our methodology on the moderated t -test introduced by Smyth *et al.* (2004). This testing technique relies on the empirical Bayes procedure, commonly used in microarray data analysis, and to a more recent extent for differential analysis in quantitative proteomics Wieczorek *et al.* (2017). The moderated t -test procedure relies on the following Bayesian hierarchical model:

$$\hat{s}_p^2 \mid \sigma_p^2 \sim \frac{\sigma_p^2}{d_p} \times \chi_{d_p}^2 \quad \text{and} \quad \frac{1}{\sigma_p^2} \sim \frac{1}{d_0 \times s_0^2} \times \chi_{d_0}^2 \quad (7)$$

where σ_p^2 is the peptide-wise variance, d_0 and s_0 are hyperparameters to be estimated (Phipson *et al.*, 2016). From there, a so-called moderated variance estimator $\hat{s}_{p[mod]}^2$ of the variance σ_p^2 is derived:

$$\hat{s}_{p[mod]}^2 = \frac{d_p \times \hat{s}_p^2 + d_0 \times s_0^2}{d_p + d_0} \quad (8)$$

This estimator is then computed in the test statistic associated to the null hypothesis $\mathcal{H}_0 : \beta_{pi} = 0$ (see Equation 9). Therefore, the results of this testing procedure account both for the specific structure of the data and the uncertainty caused by the multiple imputation step.

$$T_{pi[mod]} = \frac{\hat{\beta}_{pi}}{\hat{s}_{p[mod]}^2 \sqrt{(X^T X)_{k,k}^{-1}}} \quad (9)$$

with $(X^T \Omega_p X)_{k,k}^{-1}$ the k -th diagonal element in the matrix $(X^T \Omega_p X)^{-1}$. Under the \mathcal{H}_0 hypothesis, $T_{pi[mod]}$ follows a Student distribution with $d_p + d_0$ degrees of freedom.

As many tests as the number of peptides considered are performed. Hence, the proportion of falsely rejected hypotheses has to be controlled. Here, the False Discovery Rate control procedure from Benjamini and Hochberg (1995) was performed using the **cp4p** R package by Gai Gianetto *et al.* (2016).

3.6 Aggregation

The methodology implemented in the **mi4p** R package can be applied to peptide-level quantification data as well as protein-level quantification data. However,

we were interested in evaluating our method on a peptide-level dataset and inferring results at a protein level, as it is common practice in proteomics. Therefore, for intensity aggregation, we chose to sum all unique peptides’ intensities for each protein. The detailed pipeline for intensity aggregation is described in Supplementary data in Section S2.

3.7 Measures of performance

We compared our methodology to the `limma` testing pipeline implemented in the state-of-the-art `ProStaR` software, through the `DAPAR R` package. To assess the performances of both methods, we used the following measures: sensitivity (also known as true positive rate or recall), specificity (also known as true negative rate), precision (also known as positive predictive value), F -score and Matthews correlation coefficient. In our work, we define a true positive (respectively negative) as a peptide/protein that is correctly considered as (not) differentially expressed by the testing procedure. Similarly, we define a false positive (respectively negative) as a peptide/protein that is falsely considered as (not) differentially expressed by the testing procedure. The expressions of the previously mentioned performance indicators are given in Supplementary data in Section S3.

4 Results and Discussion

We highlight here results obtained using the maximum likelihood estimation imputation method. Results from other imputation methods on simulated data can be found in Supplementary data (Tables S4.3 to S4.6, S5.8 to S5.11 and S6.13 to S6.16). For each experiment, simulated or real, the performances of each method are based on adjusted p -values, with a 5% significance level and using a 1% Benjamini-Hochberg False Discovery Rate.

4.1 Simulated datasets

Figure 3 describes the evolution of the distribution of differences in sensitivity and specificity between `mi4p` and `DAPAR` depending on the proportion of missing values in the first set of simulations. For a small proportion of missing values (1%), where the imputation process induces little variability, performances in terms of sensitivity, specificity and F -Score are equivalent between both methods. No improvement nor deterioration was observed for sensitivity, as it remains at 100% regardless of the missing value proportion. Specificity and F -Score are improved with the `mi4p` workflow above 5% missing values. The same observations can be drawn for precision and Matthews coefficient correlation (see Figure S4.1 in Supplementary data). Detailed results can be found in Table S4.2.

Figure 4 describes the evolution of the distribution of differences in sensitivity and specificity between `mi4p` and `DAPAR` depending on the proportion of

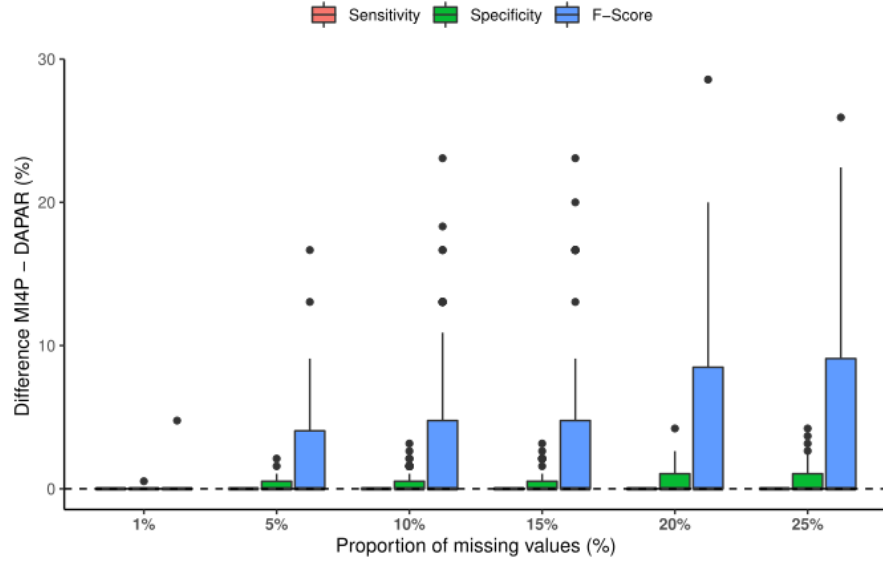


Figure 3: Distributions of differences in sensitivity, specificity and F-score for the first set of simulations.

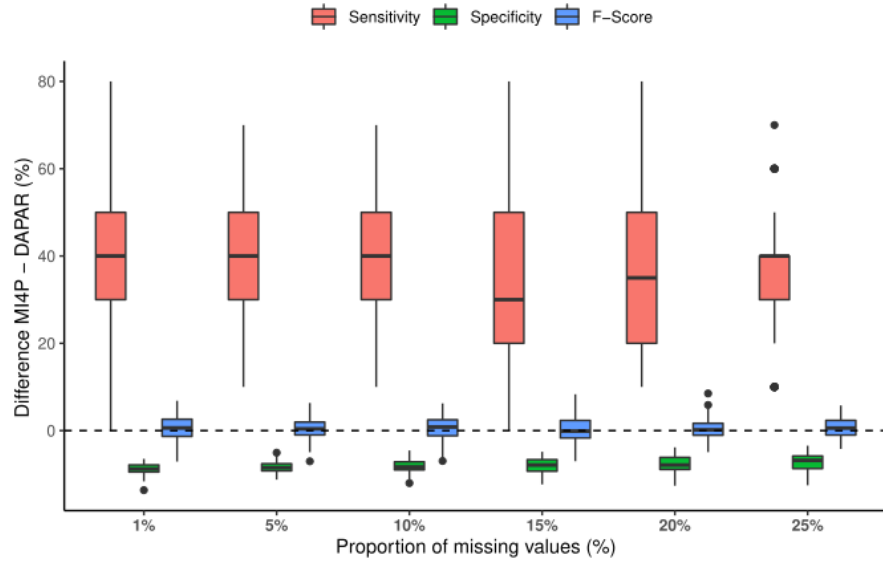


Figure 4: Distributions of differences in sensitivity, specificity and F-score for the second set of simulations.

missing values in the second set of simulations. For all proportions of missing values, we observe a trade-off between sensitivity and specificity. A slight loss in specificity (remaining above 99%) provides a greater gain in terms of sensitivity. The mean F -score across the 100 datasets is also increased with the **mi4p** workflow than with the **DAPAR** one. The Matthews correlation coefficient highlights the gain in performances (as illustrated in Supplementary data, Figure S5.2).

Extending the simulation model from fixed effects to random effects using the last set of simulations provides similar results, as shown in Supplementary data (Figure S6.3 and Tables S6.12 to S6.16).

4.2 Real datasets

The trade-off suggested by the simulation study is confirmed by the results obtained on the real datasets. In the *Saccharomyces cerevisiae* + UPS1 experiment, a decrease of 70% in the number of false positives is observed, improving the specificity and precision (Table S8.23 in Supplementary data). However, this costs in the number of true positives (see Table 2), decreasing of sensitivity. The same trend is observed in the *Arabidopsis thaliana* + UPS1 experiment; the number of false positives is decreased by 50% (see Table 3 and Table S8.17), thus improving specificity and precision at the cost of sensitivity. The loss in sensitivity is bigger in the highest points of the range in both experiments. The structure of the calibrated datasets used here can explain these observations. Indeed, the quantitative dataset considered takes into account all samples from all conditions, while the testing procedure focuses on one-vs-one comparisons. Two issues can be raised:

- The data preprocessing step can lead to more data filtering than necessary. For instance, we chose to use the filtering criterion such that rows with at least one quantified value in each condition were kept. The more conditions are considered, the more stringent the rule is, possibly leading to a poorer dataset (with fewer observations) for the conditions of interest.
- The imputation process is done on the whole dataset, as well as the estimation step. Then, while projecting the variance-covariance matrix, the estimated variance (later used in the test statistic) is the same for all comparisons. Thus, if one is interested in comparing conditions with fewer missing values, the variance estimator will be penalised by the presence of conditions with more missing values in the initial dataset.

This phenomenon is illustrated in Table S8.18, where solely the two highest points of the range have been compared, only using the quantitative data from those two conditions. More peptides have been taken into account for the statistical analysis. This strategy leads to better scores for precision, F -score and Matthews correlation coefficient compared to the previous framework.

As far as data extracted without the Match Between Runs algorithm are concerned, the results were equivalent in both methods considered in the *Arabidopsis thaliana* + UPS1 experiment (as illustrated in Tables S8.20 and S8.21).

Condition vs. 25fmol	True positives	False positives	Sensitivity	Specificity	F-Score
0.5fmol	-2.7%	-67.2%	-2.7%	+1.6%	+53.6%
1fmol	-1.6%	-71.1%	-0.5%	+0.9%	+37.8%
2.5fmol	-3.2%	-75.8%	-3.3%	+0.7%	+26.9%
5fmol	-14.3%	-78.7%	-14.3%	+0.5%	+11.4%
10fmol	-41.9%	-75.2%	-41.9%	+0.5%	-14.4%

Table 2: Performance of the **mi4p** methodology expressed in percentage with respect to **DAPAR** workflow, on *Saccharomyces cerevisiae* + UPS1 experiment, with Match Between Runs and at least 1 out of 3 quantified values in each condition. Missing values (6%) were imputed using the maximum likelihood estimation method.

Condition vs. 10fmol	True positives	False positives	Sensitivity	Specificity	F-Score
0.05fmol	-2.3%	-43%	-2.3%	+15%	+62.7%
0.25fmol	-1.5%	-43%	-1.4%	+13.9%	+65.3%
0.5fmol	-1.5%	-50.6%	-1.4%	+10.8%	+81.4%
1.25fmol	-2.3%	-62.6%	-2.3%	+10.9%	+119.8%
2.5fmol	-25.6%	-69.3%	-25.5%	+2.4%	+45.9%
5fmol	-30.3%	-65.2%	-30.4%	+5.5%	+56.1%

Table 3: Performance of the **mi4p** methodology expressed in percentage with respect to **DAPAR** workflow, on *Arabidopsis thaliana* + UPS1 experiment, with at least 1 out of 3 quantified values in each condition. Missing values (6%) were imputed using the maximum likelihood estimation method.

Furthermore, the same observations can be drawn from datasets filtered with the criterion of a minimum of 2 out of 3 observed values in each group for the *Arabidopsis thaliana* + UPS1 experiment (Tables S8.19 and S8.21) as well as for the *Saccharomyces cerevisiae* + UPS1 experiment (Table S8.24). These observations translate a loss of global information in the dataset, as filtering criteria lead to fewer peptides considered with fewer missing values per peptide.

The **mi4p** methodology also provides better results at the protein-level (after aggregation) in terms of specificity, precision, *F*-score and Matthews correlation coefficient, with a minor loss in sensitivity (Table S8.25). In particular, a decrease of 63.2% to 80% in the number of false positives is observed with a lower loss on the number of true positives and on sensitivity (up to 2.6%) for the *Saccharomyces cerevisiae* + UPS1 experiment, as illustrated in Table 5. As far as the *Arabidopsis thaliana* + UPS1 experiment is concerned, the same trend is observed (Table S8.22). Indeed, the number of false positives is decreased by 31% to 66.8%, with a maximum loss in the number of true positives of 9.8%, as illustrated in Table 4.

Condition vs. 10fmol	True positives	False positives	Sensitivity	Specificity	F-Score
0.05fmol	0%	-27.6%	0%	+18.3%	+34.2%
0.25fmol	0%	-25.7%	0%	+18.1%	+31%
0.5fmol	0%	-31%	0%	+15.2%	+39.5%
1.25fmol	0%	-65.3%	0%	+12.1	+119.2%
2.5fmol	-2.4%	-66.8%	-2.4%	+5.8%	+88.3%
5fmol	-9.8%	-57.3%	-9.8%	+12.9%	+78.9%

Table 4: Performance of the **mi4p** methodology (with the aggregation step) expressed in percentage with respect to **DAPAR** workflow, on Arabidopsis + UPS1 experiment, with at least 1 out of 3 quantified values in each condition. Missing values were imputed using the Maximum Likelihood Estimation method.

Condition vs. 25fmol	True positives	False positives	Sensitivity	Specificity	F-Score
0.5fmol	0%	-73.3%	0%	+2.9%	+61.1%
1fmol	-2.4%	-80%	-2.4%	+2.3%	+51.4%
2.5fmol	0%	-70.4%	0%	+0.8%	+20.9%
5fmol	-2.4%	-63.2%	-2.4%	+0.5%	+11.6%
10fmol	-2.6%	-69.6%	-2.6%	+0.7%	+16.5%

Table 5: Performance of the **mi4p** methodology (with the aggregation step) expressed in percentage with respect to **DAPAR** workflow, on Yeast + UPS1 experiment, with at least 1 out of 3 quantified values in each condition. Missing values were imputed using the Maximum Likelihood Estimation method.

5 Conclusion

In this work, we presented as a key step of a workflow a rigorous multiple imputation method by estimating both the parameters of interest and their variability. We considered this variability downstream of the statistical analysis by including it in the moderated t -test statistic. The methodology was implemented in the R statistical language through a package called `mi4p`. Its performance was compared on both simulated and real datasets to the state-of-the-art methodologies, such as the package `DAPAR`, using confusion matrix-based indicators. The results showed a trade-off between those indicators. In real datasets, the methodology reduces the number of false positives in exchange for a minor reduction of the number of true positives. The results are similar among all imputation methods considered, especially when the proportion of missing values is small. Our methodology with an additional aggregation step provides better results with a minor loss in sensitivity and can be of interest for proteomicists who will benefit from results at the protein level while using peptide-level quantification data.

Acknowledgements

The authors wish to thank Leslie Muller and Nicolas Pythoud for providing the real proteomics datasets used in this work, as well as Thomas Burger and Quentin Gaii-Gianetto for their help on the `DAPAR` and `imp4p` R packages. The real datasets were deposited with the ProteomeXchange Consortium via the PRIDE partner repository with the dataset identifiers PXD003841 and PXD027800 (Deutsch *et al.*, 2017).

Funding

This work was funded through a PhD grant (2018-2021) awarded to MC and received by FB and CC from the Agence Nationale de la Recherche (ANR) through the Labex IRMIA [ANR-11-LABX-0055_IRMIA].

References

- Benjamini, Y., and Hochberg, Y. (1995). Controlling the False Discovery Rate: A Practical and Powerful Approach to Multiple Testing. *Journal of the Royal Statistical Society. Series B (Methodological)*. **57(1)**, 289-300
- Bolstad, B.M. *et al.* (2003). A comparison of normalization methods for high density oligonucleotide array data based on variance and bias. *Bioinformatics*. **19(2)**, 185-93.
- Bolstad, B.M. (2021). *preprocessCore: A collection of pre-processing functions*. R package version 1.54.0.

- Chang, C. *et al.* (2018) PANDA-view: an easy-to-use tool for statistical analysis and visualization of quantitative proteomics data. *Bioinformatics*, **34**(20), 3594-3596.
- Choi, M. *et al.* (2014) MSstats: an R package for statistical analysis of quantitative mass spectrometry-based proteomic experiments. *Bioinformatics*, **30**(17), 2524-2526.
- Deutsch, E. W. *et al.* (2017) The ProteomeXchange consortium in 2017: supporting the cultural change in proteomics public data deposition. *Nucleic Acids Res.* **45**.
- Giai Gianetto, Q. *et al.* (2016) Calibration plot for proteomics: A graphical tool to visually check the assumptions underlying FDR control in quantitative experiments. *Proteomics*, **16**(1), 29-32.
- Giai Gianetto, Q. *et al.* (2020) A peptide-level multiple imputation strategy accounting for the different natures of missing values in proteomics data. bioRxiv 2020.05.29.122770; doi: <https://doi.org/10.1101/2020.05.29.122770>
- Goeminne, L.J.E. *et al.* (2015) Summarization vs Peptide-Based Models in Label-Free Quantitative Proteomics: Performance, Pitfalls, and Data Analysis Guidelines. *Journal of Proteome Research*, **14**(6), 2457-2465.
- Goeminne, L.J.E. *et al.* (2016) Peptide-level Robust Ridge Regression Improves Estimation, Sensitivity, and Specificity in Data-dependent Quantitative Label-free Shotgun Proteomics. *Molecular & Cellular Proteomics*, **15**, 657-667.
- Goeminne, L.J.E. *et al.* (2018) Experimental design and data-analysis in label-free quantitative LC/MS proteomics: A tutorial with MSqRob. *Journal of Proteomics*, **71**, 23-36.
- Goeminne, L.J.E. *et al.* (2020) MSqRob takes the missing hurdle: uniting intensity- and count-based proteomics. *Analytical Chemistry*, **92**(9), 6278-6287.
- Hardle, W.K. *et al.* (2015) *Applied Multivariate Statistical Analysis*, 4th edition, Springer.
- Hastie, T. *et al.* (1999). Imputing Missing Data for Gene Expression Arrays, Statistics Department Technical Report, Stanford University.
- Hastie, T. *et al.* (2021). *impute: Imputation for microarray data*. R package version 1.66.0.
- von Hippel, P.T. (2018). How Many Imputations Do You Need? A Two-stage Calculation Using a Quadratic Rule. *Sociological Methods & Research*, 1-20.
- Jin, L. *et al.*, (2021). A comparative study of evaluating missing value imputation methods in label-free proteomics. *Scientific Reports*, **11**, 1760.

- Josse J and Husson F. (2013). Handling missing values in exploratory multivariate data analysis methods. *Journal de la SFDS*. **153(2)**, pp. 79-99.
- Karpievitch *et al.* (2012). Normalization and missing value imputation for label-free LC-MS analysis. *BMC Bioinformatics*. **13(16)**.
- Lazar, C. *et al.* (2016) Accounting for the Multiple Natures of Missing Values in Label-Free Quantitative Proteomics Data Sets to Compare Imputation Strategies. *Journal of Proteome Research*, **15(4)**, 1116-1125.
- Little, R.J.A. and Rubin, D.B. (2019) *Statistical Analysis with missing data, 3rd edition*, John Wiley & Sons.
- Liu, M. and Dongre, A. (2020). Proper imputation of missing values in proteomics datasets for differential expression analysis. *Briefings in Bioinformatics*, **22(3)**, bbaa112.
- Muller, L. *et al.* (2016) Benchmarking sample preparation/digestion protocols reveals tube-gel being a fast and repeatable method for quantitative proteomics. *Proteomics*, **16(23)**, 2953-2961.
- Pan, Q. *et al.* (2018) Improved methods for estimating fraction of missing information in multiple imputation. *Cogent Mathematics & Statistics*, **5(1)**.
- Phipson, B. *et al.* (2016) Robust hyperparameter estimation protects against hypervariable genes and improves power to detect differential expression. *Annals of Applied Statistics*, **10(2)**, 946-963.
- Rubin, D.B. (1987). *Multiple Imputation for Nonresponse in Surveys*. John Wiley & Sons Inc., New York.
- Schafer, J.L. (1997). *Analysis of Incomplete Multivariate Data (1st ed.)*. Chapman and Hall/CRC.
- Song, J. and Yu, C. (2021) Missing Value Imputation using XGboost for Label-Free Mass Spectrometry-Based Proteomics Data. *bioRxiv* 2021.04.08.438945; doi: <https://doi.org/10.1101/2021.04.08.438945>
- Smyth, G.K. *et al.* (2004) Linear Models and Empirical Bayes Methods for Assessing Differential Expression in Microarray Experiments. *Statistical Applications in Genetics and Molecular Biology*, **3(1)**.
- Stekhoven, D.J. and Bühlmann, P. (2012). MissForest—non-parametric missing value imputation for mixed-type data. *Bioinformatics*, **28(1)**, 112–118.
- Suomi, T. *et al.* (2015) Using Peptide-Level Proteomics Data for Detecting Differentially Expressed Proteins. *Journal of Proteome Research*, **14(11)**, 4564–4570.
- Troyanskaya, O. *et al.* (2001). Missing value estimation methods for DNA microarrays. *Bioinformatics*. **17(6)**, 520-525.

- Tyanova, S. *et al.* (2016) The Perseus computational platform for comprehensive analysis of (prote)omics data. *Nature Methods*, **13**(9), 731-740.
- Van Buuren, S. and Groothuis-Oudshoorn, K. (2011). mice: Multivariate Imputation by Chained Equations in R. *Journal of Statistical Software*, **45**(3), 1-67.
- Wang, J. *et al.* (2017) In-depth method assessments of differentially expressed protein detection for shotgun proteomics data with missing values. *Scientific Reports*, **7**.
- Wang, M. *et al.* (2021). RobNorm: model-based robust normalization method for labeled quantitative mass spectrometry proteomics data. *Bioinformatics*, **37**(6), 815–821.
- White, I. R., Royston, P. and Wood, A. M. (2011) Multiple imputation using chained equations: Issues and guidance for practice. *Statistics in Medicine*, **30**, 377-399.
- Wieczorek, S. *et al.* (2017) DAPAR & ProStaR: software to perform statistical analyses in quantitative discovery proteomics. *Bioinformatics*, **33**(1), 135-136.

Supplemental Information for Accounting for multiple imputation-induced variability for differential analysis in mass spectrometry-based label-free quantitative proteomics

Marie Chion, Christine Carapito & Frédéric Bertrand

Contents

S1 State of the art on imputation in quantitative proteomics	4
S2 Aggregation of peptides' intensities	8
S3 Indicators of performance	8
S4 Results on the first set of simulations	9
S4.1 Simulation design	9
S4.2 Performance evaluation	10
S5 Results on the second set of simulations	16
S5.1 Simulation design	16
S5.2 Performance evaluation	17
S6 Results on the third set of simulations	23
S6.1 Simulation design	23
S6.2 Performance evaluation	24
S7 Real datasets generation	30
S7.1 Complex total cell lysates (<i>Saccharomyces cerevisiae</i> and <i>Arabidopsis thaliana</i>) spiked UPS1 standard protein mixtures	30
S7.2 Data preprocessing	30
S7.3 Supplemental methods for <i>Arabidopsis thaliana</i> dataset	31
S8 Results on real datasets	31
S8.1 <i>Arabidopsis thaliana</i> + UPS1 experiment	31
S8.2 <i>Saccharomyces cerevisiae</i> + UPS1 experiment	37

List of Figures

S4.1	Distribution of the difference of performance between mi4p and DAPAR workflows on the first set of simulations imputed using maximum likelihood estimation.	10
S5.2	Distribution of the difference of performance between mi4p and DAPAR workflows on the second set of simulations imputed using maximum likelihood estimation.	17
S6.3	Distribution of the difference of performance between mi4p and DAPAR workflows on the third set of simulations imputed using maximum likelihood estimation.	24

List of Tables

S1.1	State of the art on imputation methods used in quantitative proteomics and type of data used.	7
S4.2	Performance evaluation on the first set of simulations imputed using maximum likelihood estimation.	11
S4.3	Performance evaluation on the first set of simulations imputed using k -nearest neighbours.	12
S4.4	Performance evaluation on the first set of simulations imputed using Bayesian linear regression.	13
S4.5	Performance evaluation on the first set of simulations imputed using principal component analysis.	14
S4.6	Performance evaluation on the first set of simulations imputed using random forests.	15
S5.7	Performance evaluation on the second set of simulations imputed using maximum likelihood estimation.	18
S5.8	Performance evaluation on the second set of simulations imputed using k -nearest neighbours method.	19
S5.9	Performance evaluation on the second set of simulations imputed using Bayesian linear regression.	20
S5.10	Performance evaluation on the second set of simulations imputed using principal component analysis.	21
S5.11	Performance evaluation on the second set of simulations imputed using random forests.	22
S6.12	Performance evaluation on the third set of simulation imputed using maximum likelihood estimation	25
S6.13	Performance evaluation on the third set of simulations imputed using k -nearest neighbours method.	26
S6.14	Performance evaluation on the third set of simulation imputed using Bayesian linear regression.	27
S6.15	Performance evaluation on the third set of simulation imputed using principal component analysis.	28
S6.16	Performance evaluation on the third set of simulation imputed using random forests.	29

S8.17	Performance evaluation on the <i>Arabidopsis thaliana</i> + UPS1 dataset, filtered with at least 1 quantified value in each condition.	32
S8.18	Performance evaluation on the <i>Arabidopsis thaliana</i> + UPS1 dataset, filtered with at least 1 quantified value in each condition and focusing only on the comparison 5fmol vs. 10fmol. . .	32
S8.19	Performance evaluation on the <i>Arabidopsis thaliana</i> + UPS1 dataset, filtered with at least 2 quantified values in each condition.	33
S8.20	Performance evaluation on the <i>Arabidopsis thaliana</i> + UPS1 dataset, extracted without Match Between Runs and filtered with at least 1 quantified value in each condition.	34
S8.21	Performance evaluation on the <i>Arabidopsis thaliana</i> + UPS1 dataset, extracted without Match Between Runs and filtered with at least 2 quantified values in each condition.	35
S8.22	Performance evaluation on the <i>Arabidopsis thaliana</i> + UPS1 dataset at the protein-level, filtered with at least 1 quantified values in each condition.	36
S8.23	Performance evaluation on the <i>Saccharomyces cerevisiae</i> + UPS1 dataset, filtered with at least 1 quantified value in each condition.	37
S8.24	Performance evaluation on the <i>Saccharomyces cerevisiae</i> + UPS1 dataset, filtered with at least 2 quantified values in each condition.	38
S8.25	Performance evaluation on the <i>Saccharomyces cerevisiae</i> + UPS1 dataset, at the protein-level and filtered with at least 1 quantified values in each condition.	39

S1 State of the art on imputation in quantitative proteomics

Table S1.1 gives an overview of the recent literature on imputation methods in quantitative proteomics. Imputation methods are abbreviated as follows.

- **BPCA:** Bayesian principal component analysis
- **CAM:** Convex analysis of mixtures
- **FCS:** Fully conditional specification
- **FRMF:** Fused regularisation matrix factorisation
- **kNN:** k-nearest neighbours
- **LLS:** Local least-squares
- **LOD1:** Half of the global minimum
- **LOD2:** Half of the peptide minimum
- **LSA:** Least-squares adaptive
- **MBI:** Model-based imputation
- **MCMC:** Monte-Carlo Markov chains
- **MI:** Multiple imputation
- **mice:** Multiple imputation using chained equations
- **MinDet:** Deterministic minimum
- **MinProb:** Probabilistic minimum
- **MLE:** Maximum likelihood estimation
- **NIPALS:** Non-linear estimation by iterative partial least squares
- **PCA:** Principal component analysis
- **PPCA:** Probabilistic principal component analysis
- **pwKNN:** Protein-wise k-nearest neighbours
- **QRLIC:** Quantile regression imputation of left-censored
- **SLSA:** Structured least squares algorithm
- **SVD:** Singular value decomposition
- **SVT:** Singular value thresholding

- **swKNN:** Sample-wise k-nearest neighbours
- **REM:** Regularised expectation maximisation
- **RF:** Random forests
- **RTI:** Random tail imputation

AUTHORS	METHODS	DATASETS
Karpievitch et al. [2012]	Single imputation: MLE	Simulated dataset: 10 samples, 2 groups, 1400 proteins
Choi et al. [2014]	Single imputation: Accelerated Failure Time model	
Webb-Robertson et al. [2015]	Single imputation: Single-Value Approaches (LOD1, LOD2, RTI) Local Similarity Approaches (KNN, LLS, LSA, REM, MBI) Global-Structure Approaches (PPCA and BPCA)	Real datasets: Mouse plasma + Shewanella oneidensis, 60 samples, 1518 peptides Human Plasma, 71 samples, 48 vs 23 T2D, 6729 peptides Mouse Lung, 32 samples, 6295 peptides
Tyanova et al. [2016]	Single imputation: Gaussian distribution, constant	
Lazar et al. [2016]	Single imputation: kNN, SVD, MLE, MinDet, MinProb	Simulated dataset: Karpievitch et al. [2012] 1000 peptides, 20 replicates Real dataset: Zhang et al. [2014]
Yin et al. [2016]	Multiple imputation: MCMC + FCS	Real dataset: Framingham Heart Study Offspring cohort 861 plasma proteins, 135 samples MCAR amputation on the 261 entirely observed proteins Application to 544 partially unobserved proteins (40% missing values)
Wieczorek et al. [2017]	Single imputation: kNN, MLE, BPCA, Quantile regression	
Chang et al. [2018]	Single imputation: kNN Multiple imputation: mice	
Li et al. [2020]	Single imputation: Two-step lasso method, kNN, TR-kNN, RF, DanteR, Min	

AUTHORS	METHODS	DATASETS
Goeminne et al. [2020]	Hurdle model.	Real dataset: Paulovich et al. 2010
Gianetto et al. [2020]	Multiple imputation: MI, PCA, MLE, kNN, IGCDA, RF, SLISA	Simulated dataset: Ramus et al. 2016
Liu and Dongre [2020]	Single imputation: BPCA, kNN, MinProb, MLE, QRLIC, SVD, DetMin	Real datasets: 1-4 groups, 9-56 samples, 1847-6932 proteins Available on PRIDE repositories Simulated datasets: Based on the real datasets 3 groups, 27-60 samples, 2800-3500 proteins
Jin et al. [2021]	Single imputation: left-censored methods, kNN, LLS, RF, SVD, BPCA	Real datasets: (E.coli + Yeast) + UPS, 7 groups, 56 samples Immune cell dataset, 3 vs 4 samples Amputation of complete cases
Shen et al. [2021]	Single imputation: swKNN, pwKNN, Min/2, Mean, PPCA, NIPALS, SVD, SVT, FRMF, CAM	Real dataset: Herrington et al. 2018 Amputation of complete cases from real datasets
Song and Yu [2021]	Single imputation: Xgboost, mean, kNN, BPCA, LLS, RF	Real datasets: Kinases expression of human colon and rectal cancer cell line : 65 samples, 235 kinases Proteome about the interstitial lung disease : 11 samples, random draw of 500 completely observed proteins Ovarian cancer proteome dataset : 25 samples, random draw of 400 completely observed proteins

Table S1.1: State of the art on imputation methods used in quantitative proteomics and type of data used.

S2 Aggregation of peptides' intensities

The methodology implemented in the `mi4p` R package can be applied to peptide-level quantification data as well as protein-level quantification data. However, we were interested in evaluating our method on a peptide-level dataset and inferring results at a protein level, as it is common practice in proteomics. Therefore, for intensity aggregation, we chose to sum all unique peptides' intensities for each protein. We then adjusted our pipeline as follows:

1. Out-filtration of non-unique peptides from the peptide-level quantification dataset.
2. Normalisation of the log2-transformed peptide intensities.
3. Multiple imputation of log2-transformed peptide intensities.
4. Aggregation by summing all peptides intensities (non-log2-transformed) from a given protein in each imputed dataset.
5. log2-transformation of protein intensities.
6. Estimation of variance-covariance matrix.
7. Projection of the estimated variance-covariance matrix.
8. Moderated t -testing on the combined protein-level dataset

S3 Indicators of performance

Let TP , TN , FP and FN respectively denote the numbers of true positives, true negatives, false positives, and false negatives.

$$\text{Sensitivity} = \frac{TP}{TP + FN} \quad (1)$$

$$\text{Specificity} = \frac{TN}{TN + FP} \quad (2)$$

$$\text{Precision} = \frac{TP}{TP + FP} \quad (3)$$

$$F\text{-Score} = \frac{TP}{TP + \frac{1}{2} \times (FP + FN)} \quad (4)$$

$$\text{MCC} = \frac{TP \times TN - FP \times FN}{\sqrt{(TP + FP)(TP + FN)(TN + FP)(TN + FN)}} \quad (5)$$

S4 Results on the first set of simulations

S4.1 Simulation design

We considered an experimental design where the distributions of the two groups to be compared scarcely overlap. This design led to a fixed effect one-way ANOVA model, which can be written as:

$$y_{ij} = \mu + \delta_{ij} + \epsilon_{ij} \quad (6)$$

with $\mu = 100$, $\delta_{ij} = 100$ if $1 \leq i \leq 10$ and $j = 2$ and $\delta_{ij} = 0$ otherwise and $\epsilon_{ijk} \sim \mathcal{N}(0, 1)$. Here, y_{ij} represents the log-transformed abundance of peptide i in the j -th sample. Thus, we generated 100 datasets by considering 200 individuals and 10 variables, divided into 2 groups of 5 variables, using the following steps:

1. For the first 10 rows of the data frame, set as differentially expressed, draw the first 5 observations (first group) from a Gaussian distribution with a mean of 100 and a standard deviation of 1. Then draw the remaining 5 observations (second group) from a Gaussian distribution with a mean of 200 and a standard deviation of 1.
2. For the remaining 190 rows, set as non-differentially expressed, draw the first 5 observations as well as the last 5 observations from a Gaussian distribution with a mean of 100 and a standard deviation of 1.

S4.2 Performance evaluation

This subsection provides the evaluation of the `mi4p` workflow compared to the `DAPAR` workflow on the first set of simulations. The performance is described using the indicators detailed in Section S3.

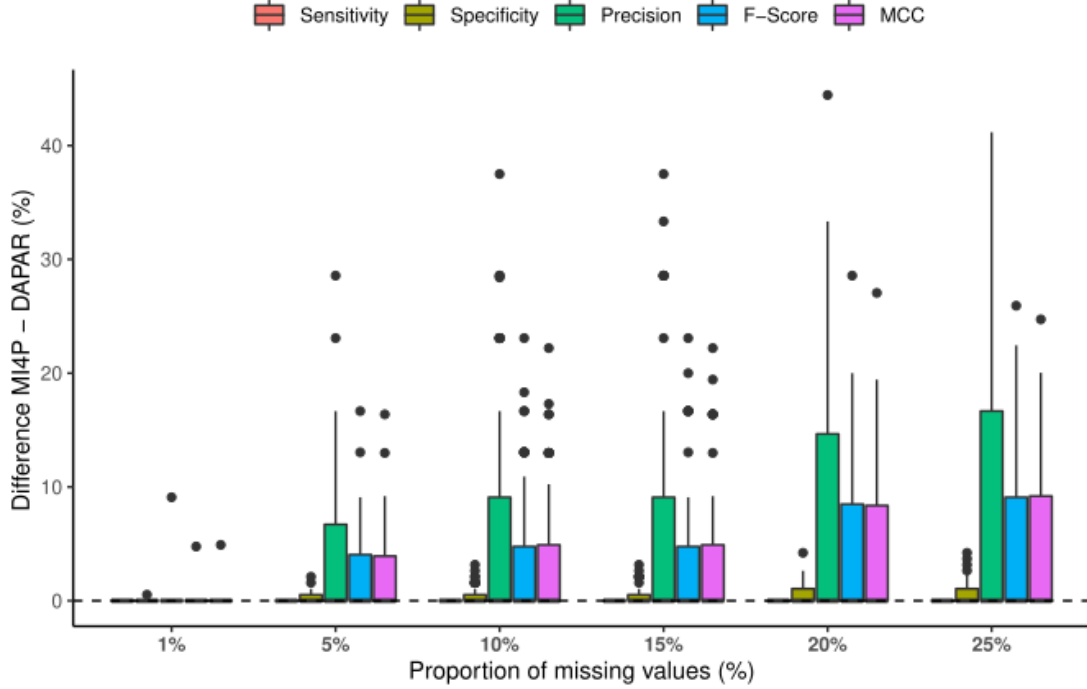


Figure S4.1: Distribution of the difference of performance between `mi4p` and `DAPAR` workflows on the first set of simulations imputed using maximum likelihood estimation.

The following tables provide results expressed as the mean of the given indicator over the 100 simulated datasets \pm the mean of the standard deviations of the given indicator over the 100 simulated datasets. Results are based on adjusted p-values using the Benjamini-Hochberg procedure [Benjamini and Hochberg, 1995] and a false discovery rate of 1%.

%MV	Method	True positives	False positives	True negatives	False negatives	Sensitivity (%)	Specificity (%)	Precision (%)	F-score (%)	MCC (%)
1%	DAPAR	10 \pm 0	0.5 \pm 0.7	189.5 \pm 0.7	0 \pm 0	100 \pm 0	99.8 \pm 0.4	95.9 \pm 5.7	97.8 \pm 3.1	97.8 \pm 3.1
	MI4P	10 \pm 0	0.5 \pm 0.7	189.5 \pm 0.7	0 \pm 0	100 \pm 0	99.8 \pm 0.4	96 \pm 5.7	97.9 \pm 3.1	97.8 \pm 3.1
5%	DAPAR	10 \pm 0	0.8 \pm 1	189.2 \pm 1	0 \pm 0	100 \pm 0	99.6 \pm 0.5	92.9 \pm 7.6	96.2 \pm 4.2	96.1 \pm 4.2
	MI4P	10 \pm 0	0.5 \pm 0.7	189.5 \pm 0.7	0 \pm 0	100 \pm 0	99.8 \pm 0.4	95.9 \pm 6.1	97.8 \pm 3.3	97.8 \pm 3.4
10%	DAPAR	10 \pm 0	1.2 \pm 1.3	188.8 \pm 1.3	0 \pm 0	100 \pm 0	99.4 \pm 0.7	90.3 \pm 9.3	94.6 \pm 5.4	94.6 \pm 5.3
	MI4P	10 \pm 0	0.6 \pm 0.8	189.4 \pm 0.8	0 \pm 0	100 \pm 0	99.7 \pm 0.4	95.3 \pm 6.8	97.5 \pm 3.7	97.4 \pm 3.8
15%	DAPAR	10 \pm 0	1.3 \pm 1.3	188.7 \pm 1.3	0 \pm 0	100 \pm 0	99.3 \pm 0.7	89.6 \pm 9.4	94.2 \pm 5.4	94.2 \pm 5.4
	MI4P	10 \pm 0	0.6 \pm 1	189.4 \pm 1	0 \pm 0	100 \pm 0	99.7 \pm 0.5	95.3 \pm 7.4	97.4 \pm 4.2	97.4 \pm 4.2
20%	DAPAR	10 \pm 0	2.2 \pm 1.7	187.7 \pm 1.7	0 \pm 0	100 \pm 0	98.8 \pm 0.9	83.1 \pm 10.9	90.4 \pm 6.6	90.5 \pm 6.4
	MI4P	10 \pm 0	1.3 \pm 1.7	188.6 \pm 1.8	0 \pm 0	100 \pm 0	99.3 \pm 0.9	89.8 \pm 11.4	94.2 \pm 6.7	94.3 \pm 6.6
25%	DAPAR	10 \pm 0.2	2.9 \pm 2.1	186.8 \pm 2.2	0 \pm 0	100 \pm 0	98.5 \pm 1.1	79.7 \pm 12.5	88.2 \pm 7.9	88.3 \pm 7.5
	MI4P	10 \pm 0.2	1.6 \pm 1.8	188 \pm 2.1	0 \pm 0	100 \pm 0	99.2 \pm 1	88.3 \pm 12	93.3 \pm 7.2	93.4 \pm 7

Table S4.2: Performance evaluation on the first set of simulations imputed using maximum likelihood estimation.

%MV	Method	True positives	False positives	True negatives	False negatives	Sensitivity (%)	Specificity (%)	Precision (%)	F-score (%)	MCC (%)
1%	DAPAR	10 \pm 0	0.4 \pm 0.6	189.6 \pm 0.6	0 \pm 0	100 \pm 0	99.8 \pm 0.3	96.3 \pm 5.4	98 \pm 2.9	98 \pm 2.9
	MI4P	10 \pm 0	0.4 \pm 0.6	189.6 \pm 0.6	0 \pm 0	100 \pm 0	99.8 \pm 0.3	96.3 \pm 5.4	98 \pm 2.9	98 \pm 2.9
5%	DAPAR	10 \pm 0	0.3 \pm 0.5	189.7 \pm 0.5	0 \pm 0	100 \pm 0	99.9 \pm 0.3	97.7 \pm 4.5	98.8 \pm 2.4	98.7 \pm 2.5
	MI4P	10 \pm 0	0.3 \pm 0.5	189.7 \pm 0.5	0 \pm 0	100 \pm 0	99.9 \pm 0.3	97.7 \pm 4.5	98.8 \pm 2.4	98.7 \pm 2.5
10%	DAPAR	10 \pm 0	0.3 \pm 0.6	189.7 \pm 0.6	0 \pm 0	100 \pm 0	99.8 \pm 0.3	97.2 \pm 4.9	98.5 \pm 2.6	98.5 \pm 2.7
	MI4P	10 \pm 0	0.3 \pm 0.6	189.7 \pm 0.6	0 \pm 0	100 \pm 0	99.8 \pm 0.3	97.2 \pm 4.9	98.5 \pm 2.6	98.5 \pm 2.7
15%	DAPAR	10 \pm 0.1	0.2 \pm 0.6	189.8 \pm 0.6	0 \pm 0.1	99.9 \pm 1	99.9 \pm 0.3	97.9 \pm 4.7	98.8 \pm 2.6	98.8 \pm 2.6
	MI4P	10 \pm 0.1	0.2 \pm 0.6	189.8 \pm 0.6	0 \pm 0.1	99.9 \pm 1	99.9 \pm 0.3	97.9 \pm 4.7	98.8 \pm 2.6	98.8 \pm 2.6
20%	DAPAR	9.9 \pm 0.2	0.4 \pm 0.7	189.6 \pm 0.7	0.1 \pm 0.2	99.4 \pm 2.4	99.8 \pm 0.4	96.2 \pm 5.8	97.6 \pm 3.3	97.6 \pm 3.3
	MI4P	9.9 \pm 0.2	0.4 \pm 0.7	189.6 \pm 0.7	0.1 \pm 0.2	99.4 \pm 2.4	99.8 \pm 0.4	96.2 \pm 5.8	97.6 \pm 3.3	97.6 \pm 3.3
25%	DAPAR	9.8 \pm 0.5	0.9 \pm 1	189.1 \pm 1	0.2 \pm 0.5	97.7 \pm 4.7	99.5 \pm 0.5	92.7 \pm 7.8	94.9 \pm 4.7	94.8 \pm 4.8
	MI4P	9.8 \pm 0.5	0.9 \pm 1	189.1 \pm 1	0.2 \pm 0.5	97.7 \pm 4.7	99.5 \pm 0.5	92.7 \pm 7.8	94.9 \pm 4.7	94.8 \pm 4.8

Table S4.3: Performance evaluation on the first set of simulations imputed using k -nearest neighbours.

%MV	Method	True positives	False positives	True negatives	False negatives	Sensitivity (%)	Specificity (%)	Precision (%)	F-score (%)	MCC (%)
1%	DAPAR	10 \pm 0.2	0.2 \pm 0.4	189.8 \pm 0.4	0 \pm 0.2	99.8 \pm 2	99.9 \pm 0.2	98.4 \pm 3.7	99 \pm 2.2	99 \pm 2.2
	MI4P	9.9 \pm 0.3	0.2 \pm 0.4	189.8 \pm 0.4	0.1 \pm 0.3	99.3 \pm 2.9	99.9 \pm 0.2	98.3 \pm 4	98.7 \pm 2.8	98.7 \pm 2.8
5%	DAPAR	10 \pm 0.2	0.2 \pm 0.4	189.8 \pm 0.4	0 \pm 0.2	99.6 \pm 2	99.9 \pm 0.2	98.6 \pm 3.7	99 \pm 2.1	99 \pm 2.2
	MI4P	9.7 \pm 0.5	0.2 \pm 0.4	189.8 \pm 0.4	0.3 \pm 0.5	96.9 \pm 5.4	99.9 \pm 0.2	97.9 \pm 4.1	97.3 \pm 3.4	97.2 \pm 3.5
10%	DAPAR	10 \pm 0	0.2 \pm 0.5	189.8 \pm 0.5	0 \pm 0	100 \pm 0	99.9 \pm 0.2	97.8 \pm 4.1	98.9 \pm 2.1	98.8 \pm 2.2
	MI4P	9.6 \pm 0.7	0.1 \pm 0.3	189.9 \pm 0.3	0.4 \pm 0.7	95.5 \pm 6.9	100 \pm 0.1	99.2 \pm 2.6	97.2 \pm 4	97.1 \pm 4
15%	DAPAR	10 \pm 0	0.3 \pm 0.6	189.7 \pm 0.6	0 \pm 0	100 \pm 0	99.8 \pm 0.3	97.2 \pm 4.9	98.5 \pm 2.6	98.5 \pm 2.7
	MI4P	9.2 \pm 0.9	0 \pm 0.2	190 \pm 0.2	0.8 \pm 0.9	91.7 \pm 8.8	100 \pm 0.1	99.6 \pm 1.8	95.3 \pm 4.9	95.3 \pm 4.8
20%	DAPAR	10 \pm 0	0.6 \pm 0.8	189.4 \pm 0.8	0 \pm 0	100 \pm 0	99.7 \pm 0.4	94.6 \pm 6.4	97.1 \pm 3.5	97.1 \pm 3.6
	MI4P	8.9 \pm 1	0 \pm 0.1	190 \pm 0.1	1.1 \pm 1	89.1 \pm 10.3	100 \pm 0.1	99.9 \pm 1	93.9 \pm 6.1	93.9 \pm 5.9
25%	DAPAR	10 \pm 0.1	1.2 \pm 1.1	188.8 \pm 1.1	0 \pm 0.1	99.9 \pm 1	99.4 \pm 0.6	90.3 \pm 8	94.7 \pm 4.6	94.6 \pm 4.6
	MI4P	8.9 \pm 1.1	0 \pm 0	190 \pm 0	1.1 \pm 1.1	89.3 \pm 11.1	100 \pm 0	100 \pm 0	94 \pm 6.7	94.1 \pm 6.4

Table S4.4: Performance evaluation on the first set of simulations imputed using Bayesian linear regression.

%MV	Method	True positives	False positives	True negatives	False negatives	Sensitivity (%)	Specificity (%)	Precision (%)	F-score (%)	MCC (%)
1%	DAPAR	10 \pm 0	0.5 \pm 0.7	189.5 \pm 0.7	0 \pm 0	100 \pm 0	99.7 \pm 0.4	95.8 \pm 6	97.8 \pm 3.3	97.7 \pm 3.3
	MI4P	10 \pm 0	0.5 \pm 0.7	189.5 \pm 0.7	0 \pm 0	100 \pm 0	99.7 \pm 0.4	95.8 \pm 6	97.8 \pm 3.3	97.7 \pm 3.3
5%	DAPAR	10 \pm 0	0.6 \pm 0.8	189.4 \pm 0.8	0 \pm 0	100 \pm 0	99.7 \pm 0.4	94.6 \pm 6.8	97.1 \pm 3.7	97 \pm 3.7
	MI4P	10 \pm 0	0.6 \pm 0.8	189.4 \pm 0.8	0 \pm 0	100 \pm 0	99.7 \pm 0.4	94.6 \pm 6.8	97.1 \pm 3.7	97 \pm 3.7
10%	DAPAR	10 \pm 0	1 \pm 1.1	189 \pm 1.1	0 \pm 0	100 \pm 0	99.5 \pm 0.6	91.8 \pm 8.3	95.5 \pm 4.7	95.5 \pm 4.7
	MI4P	10 \pm 0	1 \pm 1.1	189 \pm 1.1	0 \pm 0	100 \pm 0	99.5 \pm 0.6	91.8 \pm 8.3	95.5 \pm 4.7	95.5 \pm 4.7
15%	DAPAR	10 \pm 0	1.2 \pm 1.2	188.8 \pm 1.2	0 \pm 0	100 \pm 0	99.4 \pm 0.6	90.1 \pm 8.9	94.5 \pm 5.1	94.5 \pm 5.1
	MI4P	10 \pm 0	1.2 \pm 1.2	188.8 \pm 1.2	0 \pm 0	100 \pm 0	99.4 \pm 0.6	90.1 \pm 8.9	94.5 \pm 5.1	94.5 \pm 5.1
20%	DAPAR	10 \pm 0	1.9 \pm 1.5	188 \pm 1.5	0 \pm 0	100 \pm 0	99 \pm 0.8	85.1 \pm 9.8	91.6 \pm 5.9	91.6 \pm 5.7
	MI4P	10 \pm 0	1.9 \pm 1.5	188 \pm 1.5	0 \pm 0	100 \pm 0	99 \pm 0.8	85.4 \pm 9.8	91.8 \pm 5.9	91.8 \pm 5.7
25%	DAPAR	10 \pm 0.2	2.5 \pm 1.6	187.2 \pm 1.7	0 \pm 0	100 \pm 0	98.7 \pm 0.9	81 \pm 10.5	89.1 \pm 6.4	89.2 \pm 6.1
	MI4P	10 \pm 0.2	2.6 \pm 1.6	186.8 \pm 2	0 \pm 0	100 \pm 0	98.6 \pm 0.9	80.5 \pm 10.5	88.8 \pm 6.4	88.9 \pm 6.2

Table S4.5: Performance evaluation on the first set of simulations imputed using principal component analysis.

%MV	Method	True positives	False positives	True negatives	False negatives	Sensitivity (%)	Specificity (%)	Precision (%)	F-score (%)	MCC (%)
1%	DAPAR	10 \pm 0	0.5 \pm 0.7	189.5 \pm 0.7	0 \pm 0	100 \pm 0	99.8 \pm 0.4	96 \pm 6	97.9 \pm 3.3	97.8 \pm 3.3
	MI4P	10 \pm 0	0.5 \pm 0.7	189.5 \pm 0.7	0 \pm 0	100 \pm 0	99.8 \pm 0.4	96 \pm 6	97.9 \pm 3.3	97.8 \pm 3.3
5%	DAPAR	10 \pm 0	0.4 \pm 0.6	189.6 \pm 0.6	0 \pm 0	100 \pm 0	99.8 \pm 0.3	96 \pm 5.3	97.9 \pm 2.8	97.8 \pm 2.9
	MI4P	10 \pm 0	0.4 \pm 0.6	189.6 \pm 0.6	0 \pm 0	100 \pm 0	99.8 \pm 0.3	96 \pm 5.3	97.9 \pm 2.8	97.8 \pm 2.9
10%	DAPAR	10 \pm 0	0.5 \pm 0.8	189.5 \pm 0.8	0 \pm 0	100 \pm 0	99.7 \pm 0.4	95.8 \pm 6.7	97.7 \pm 3.7	97.7 \pm 3.7
	MI4P	10 \pm 0.1	0.5 \pm 0.8	189.5 \pm 0.8	0 \pm 0.1	99.8 \pm 1.4	99.7 \pm 0.4	95.9 \pm 6.4	97.7 \pm 3.6	97.6 \pm 3.6
15%	DAPAR	10 \pm 0	0.3 \pm 0.6	189.7 \pm 0.6	0 \pm 0	100 \pm 0	99.8 \pm 0.3	97.2 \pm 5.3	98.5 \pm 2.9	98.5 \pm 2.9
	MI4P	10 \pm 0.1	0.4 \pm 0.7	189.6 \pm 0.7	0 \pm 0.1	99.8 \pm 1.4	99.8 \pm 0.3	96.8 \pm 5.5	98.2 \pm 3	98.1 \pm 3
20%	DAPAR	10 \pm 0.1	0.4 \pm 0.6	189.5 \pm 0.7	0 \pm 0.1	99.8 \pm 1.4	99.8 \pm 0.3	96.3 \pm 5.4	97.9 \pm 3	97.9 \pm 3.1
	MI4P	10 \pm 0.1	0.4 \pm 0.6	189.4 \pm 0.8	0 \pm 0.1	99.8 \pm 1.4	99.8 \pm 0.3	96 \pm 5.4	97.8 \pm 3	97.7 \pm 3.1
25%	DAPAR	10 \pm 0.2	0.3 \pm 0.6	189.4 \pm 0.9	0 \pm 0.1	99.9 \pm 1	99.8 \pm 0.3	97.5 \pm 5	98.6 \pm 2.7	98.6 \pm 2.8
	MI4P	9.9 \pm 0.2	0.3 \pm 0.6	189.1 \pm 1.3	0 \pm 0.2	99.7 \pm 1.7	99.9 \pm 0.3	97.5 \pm 4.9	98.5 \pm 2.7	98.5 \pm 2.8

Table S4.6: Performance evaluation on the first set of simulations imputed using random forests.

S5 Results on the second set of simulations

S5.1 Simulation design

Secondly, we considered an experimental design, where the distributions of the two groups to be compared might highly overlap. Hence, we based it on the random hierarchical ANOVA model by Lazar et al. [2016], derived from Karpievitch et al. [2012]. The simulation design follows the following model:

$$y_{ij} = P_i + G_{ik} + \epsilon_{ijk} \quad (7)$$

where y_{ij} is the log-transformed abundance of peptide i in the j -th sample, P_i is the mean value of peptide i , G_{ik} is the mean difference between the condition groups, and ϵ_{ijk} is the random error term, which stands for the peptide-wise variance. We generated 100 datasets by considering 1000 individuals and 20 variables, divided into 2 groups of 10 variables, using the following steps:

1. Generate the peptide-wise effect P_i by drawing 1000 observations from a Gaussian distribution with a mean of 1.5 and a standard deviation of 0.5.
2. Generate the group effect G_{ik} by drawing 200 observations (for the 200 individuals set as differentially expressed) from a Gaussian distribution with a mean of 1.5 and a standard deviation of 0.5 and 800 observations fixed to 0.
3. Build the first group dataset by replicating 10 times the sum of P_i and the random error term, drawn from a Gaussian distribution of mean 0 and standard deviation 0.5.
4. Build the second group dataset by replicating 10 times the sum of P_i , G_{ik} and the random error term drawn from a Gaussian distribution of mean 0 and standard deviation 0.5.
5. Bind both datasets to get the complete dataset.

S5.2 Performance evaluation

This subsection provides the evaluation of the **mi4p** workflow compared to the **DAPAR** workflow on the second set of simulations. The performance is described using the indicators detailed in Section S3.

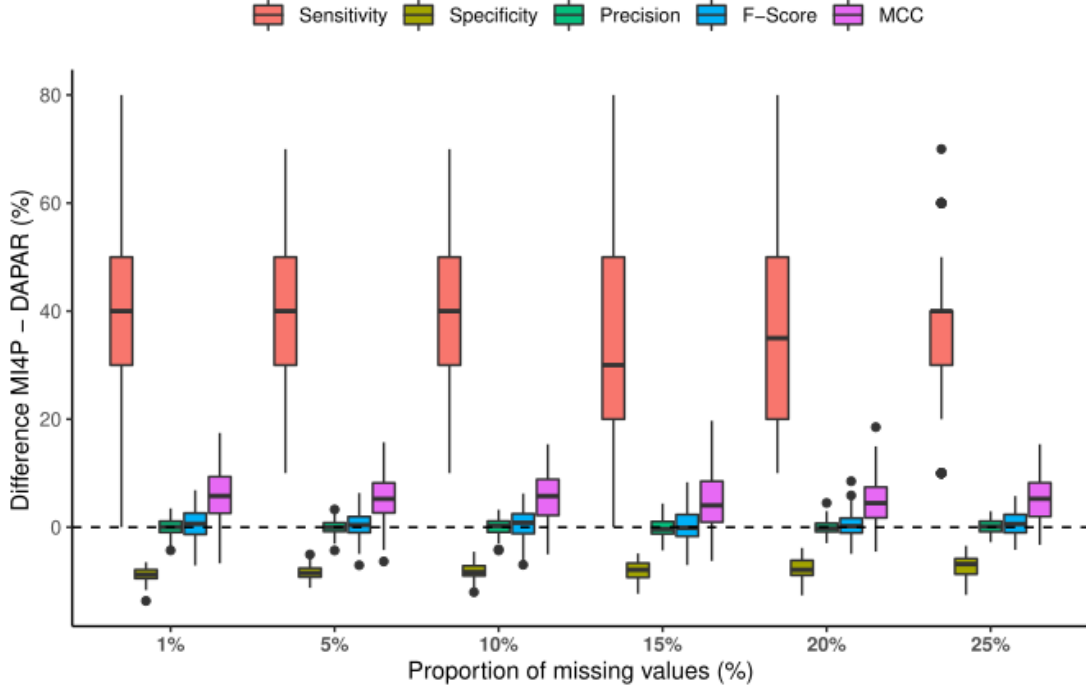


Figure S5.2: Distribution of the difference of performance between **mi4p** and **DAPAR** workflows on the second set of simulations imputed using maximum likelihood estimation.

The following tables provide results expressed as the mean of the given indicator over the 100 simulated datasets \pm the mean of the standard deviations of the given indicator over the 100 simulated datasets. Results are based on adjusted p-values using the Benjamini-Hochberg procedure [Benjamini and Hochberg, 1995] and a false discovery rate of 1%.

%MV	Method	True positives	False positives	True negatives	False negatives	Sensitivity (%)	Specificity (%)	Precision (%)	F-score (%)	MCC (%)
1%	DAPAR	80.8 \pm 11.4	1.9 \pm 1.5	798.1 \pm 1.5	119.2 \pm 11.4	40.4 \pm 5.7	99.8 \pm 0.2	97.8 \pm 1.6	56.9 \pm 5.9	58.2 \pm 4.5
	MI4P	166.9 \pm 5	6.3 \pm 2.7	793.7 \pm 2.7	33.1 \pm 5	83.4 \pm 2.5	99.2 \pm 0.3	96.4 \pm 1.4	89.4 \pm 1.5	87.4 \pm 1.6
5%	DAPAR	80.8 \pm 12.1	2.4 \pm 1.8	797.6 \pm 1.8	119.2 \pm 12.1	40.4 \pm 6.1	99.7 \pm 0.2	97.3 \pm 1.9	56.8 \pm 6.1	58 \pm 4.6
	MI4P	164.2 \pm 6.1	6.1 \pm 3.5	793.9 \pm 3.5	35.8 \pm 6.1	82.1 \pm 3	99.2 \pm 0.4	96.5 \pm 1.9	88.7 \pm 1.5	86.6 \pm 1.6
10%	DAPAR	78.8 \pm 11.9	2.4 \pm 1.6	797.6 \pm 1.6	121.2 \pm 11.9	39.4 \pm 5.9	99.7 \pm 0.2	97.1 \pm 1.8	55.8 \pm 6.1	57.1 \pm 4.7
	MI4P	160.7 \pm 7.8	5.6 \pm 3.8	794.4 \pm 3.8	39.3 \pm 7.8	80.4 \pm 3.9	99.3 \pm 0.5	96.7 \pm 2.1	87.7 \pm 1.9	85.6 \pm 2
15%	DAPAR	80.3 \pm 11.4	3.3 \pm 1.9	796.7 \pm 1.9	119.7 \pm 11.4	40.1 \pm 5.7	99.6 \pm 0.2	96.1 \pm 2.1	56.4 \pm 5.8	57.3 \pm 4.6
	MI4P	159 \pm 8.8	6.7 \pm 5.1	793.3 \pm 5.1	41 \pm 8.8	79.5 \pm 4.4	99.2 \pm 0.6	96.2 \pm 2.7	86.9 \pm 2.1	84.7 \pm 2.2
20%	DAPAR	81.3 \pm 11.6	4 \pm 2.1	796 \pm 2.1	118.7 \pm 11.6	40.7 \pm 5.8	99.5 \pm 0.3	95.4 \pm 2.4	56.8 \pm 5.9	57.4 \pm 4.7
	MI4P	158 \pm 9.8	7.2 \pm 5.4	792.8 \pm 5.4	42 \pm 9.8	79 \pm 4.9	99.1 \pm 0.7	95.8 \pm 2.9	86.5 \pm 2.3	84.2 \pm 2.3
25%	DAPAR	82.5 \pm 12.3	4.7 \pm 2.7	795.3 \pm 2.7	117.5 \pm 12.3	41.2 \pm 6.2	99.4 \pm 0.3	94.7 \pm 2.8	57.2 \pm 6	57.5 \pm 4.8
	MI4P	154.5 \pm 10.4	6.9 \pm 6.2	793.1 \pm 6.2	45.5 \pm 10.4	77.3 \pm 5.2	99.1 \pm 0.8	96 \pm 3.3	85.4 \pm 2.5	83.1 \pm 2.4

Table S5.7: Performance evaluation on the second set of simulations imputed using maximum likelihood estimation.

%MV	Method	True positives	False positives	True negatives	False negatives	Sensitivity (%)	Specificity (%)	Precision (%)	F-score (%)	MCC (%)
1%	DAPAR	80.5 \pm 12.1	1.8 \pm 1.4	798.2 \pm 1.4	119.5 \pm 12.1	40.2 \pm 6	99.8 \pm 0.2	97.9 \pm 1.6	56.8 \pm 6.3	58.1 \pm 4.9
	MI4P	167.9 \pm 4.8	6.6 \pm 2.5	793.4 \pm 2.5	32 \pm 4.8	84 \pm 2.4	99.2 \pm 0.3	96.2 \pm 1.4	89.7 \pm 1.4	87.6 \pm 1.7
5%	DAPAR	79.6 \pm 12.4	1.9 \pm 1.7	798.1 \pm 1.7	120.4 \pm 12.4	39.8 \pm 6.2	99.8 \pm 0.2	97.8 \pm 1.9	56.2 \pm 6.5	57.7 \pm 5
	MI4P	169.6 \pm 4.3	6.7 \pm 2.8	793.3 \pm 2.8	30.4 \pm 4.3	84.8 \pm 2.2	99.2 \pm 0.4	96.2 \pm 1.5	90.1 \pm 1.4	88.1 \pm 1.6
10%	DAPAR	78.2 \pm 13.5	2 \pm 1.7	798 \pm 1.7	121.8 \pm 13.5	39.1 \pm 6.8	99.8 \pm 0.2	97.7 \pm 1.8	55.5 \pm 7.1	57.1 \pm 5.4
	MI4P	170.8 \pm 4.3	6.3 \pm 2.8	793.7 \pm 2.8	29.2 \pm 4.3	85.4 \pm 2.2	99.2 \pm 0.4	96.5 \pm 1.5	90.6 \pm 1.4	88.7 \pm 1.6
15%	DAPAR	79 \pm 14.1	2 \pm 1.7	798 \pm 1.7	121 \pm 14.1	39.5 \pm 7	99.8 \pm 0.2	97.6 \pm 1.8	55.9 \pm 7.3	57.4 \pm 5.6
	MI4P	171.6 \pm 4.5	6.2 \pm 3.1	793.8 \pm 3.1	28.4 \pm 4.5	85.8 \pm 2.2	99.2 \pm 0.4	96.5 \pm 1.7	90.8 \pm 1.4	89 \pm 1.7
20%	DAPAR	77.2 \pm 16.8	1.9 \pm 1.6	798.1 \pm 1.6	122.8 \pm 16.8	38.6 \pm 8.4	99.8 \pm 0.2	97.7 \pm 1.9	54.7 \pm 9.8	56.4 \pm 7.9
	MI4P	171.1 \pm 4.7	5.7 \pm 2.7	794.3 \pm 2.7	28.9 \pm 4.7	85.5 \pm 2.3	99.3 \pm 0.3	96.8 \pm 1.5	90.8 \pm 1.4	89 \pm 1.7
25%	DAPAR	74.4 \pm 16.8	1.8 \pm 1.7	798.2 \pm 1.7	125.6 \pm 16.8	37.2 \pm 8.4	99.8 \pm 0.2	97.7 \pm 1.9	53.3 \pm 9.8	55.3 \pm 7.8
	MI4P	170.3 \pm 4.9	5.9 \pm 2.9	794.1 \pm 2.9	29.7 \pm 4.9	85.1 \pm 2.5	99.3 \pm 0.4	96.7 \pm 1.6	90.5 \pm 1.5	88.6 \pm 1.8

Table S5.8: Performance evaluation on the second set of simulations imputed using k -nearest neighbours method.

%MV	Method	True positives	False positives	True negatives	False negatives	Sensitivity (%)	Specificity (%)	Precision (%)	F-score (%)	MCC (%)
1%	DAPAR	80.7 \pm 11.9	1.9 \pm 1.6	798.1 \pm 1.6	119.3 \pm 11.9	40.4 \pm 6	99.8 \pm 0.2	97.8 \pm 1.8	56.8 \pm 6.1	58.2 \pm 4.7
	MI4P	165.7 \pm 5	5.4 \pm 2.4	794.6 \pm 2.4	34.3 \pm 5	82.8 \pm 2.5	99.3 \pm 0.3	96.9 \pm 1.3	89.3 \pm 1.5	87.3 \pm 1.7
5%	DAPAR	80.5 \pm 12.5	2.3 \pm 1.7	797.7 \pm 1.7	119.5 \pm 12.5	40.3 \pm 6.2	99.7 \pm 0.2	97.3 \pm 1.8	56.6 \pm 6.4	57.9 \pm 4.9
	MI4P	157.3 \pm 5.5	2.5 \pm 1.7	797.5 \pm 1.7	42.6 \pm 5.5	78.7 \pm 2.8	99.7 \pm 0.2	98.5 \pm 1	87.4 \pm 1.7	85.5 \pm 1.7
10%	DAPAR	79.6 \pm 12.8	2.7 \pm 2	797.3 \pm 2	120.4 \pm 12.8	39.8 \pm 6.4	99.7 \pm 0.2	96.9 \pm 2.1	56.1 \pm 6.5	57.3 \pm 5
	MI4P	156.2 \pm 5.7	2.4 \pm 1.6	797.6 \pm 1.6	43.8 \pm 5.7	78.1 \pm 2.8	99.7 \pm 0.2	98.5 \pm 1	87.1 \pm 1.8	85.2 \pm 1.9
15%	DAPAR	80.6 \pm 15	3.2 \pm 2.4	796.8 \pm 2.4	119.4 \pm 15	40.3 \pm 7.5	99.6 \pm 0.3	96.3 \pm 2.5	56.3 \pm 8.3	57.3 \pm 6.6
	MI4P	150.7 \pm 6.7	1.6 \pm 1.2	798.4 \pm 1.2	49.3 \pm 6.7	75.3 \pm 3.4	99.8 \pm 0.1	98.9 \pm 0.8	85.5 \pm 2.2	83.6 \pm 2.2
20%	DAPAR	80.5 \pm 15.3	3.9 \pm 2.6	796.1 \pm 2.6	119.5 \pm 15.3	40.3 \pm 7.6	99.5 \pm 0.3	95.5 \pm 2.7	56.2 \pm 8.1	57 \pm 6.3
	MI4P	144 \pm 6.9	0.9 \pm 1	799.1 \pm 1	56 \pm 6.9	72 \pm 3.4	99.9 \pm 0.1	99.4 \pm 0.7	83.4 \pm 2.3	81.7 \pm 2.3
25%	DAPAR	79.7 \pm 17.6	4.6 \pm 3.2	795.4 \pm 3.2	120.3 \pm 17.6	39.9 \pm 8.8	99.4 \pm 0.4	94.8 \pm 2.8	55.5 \pm 9.5	56.3 \pm 7.3
	MI4P	137.2 \pm 6.7	0.6 \pm 0.8	799.4 \pm 0.8	62.8 \pm 6.7	68.6 \pm 3.3	99.9 \pm 0.1	99.6 \pm 0.6	81.2 \pm 2.4	79.5 \pm 2.3

Table S5.9: Performance evaluation on the second set of simulations imputed using Bayesian linear regression.

%MV	Method	True positives	False positives	True negatives	False negatives	Sensitivity (%)	Specificity (%)	Precision (%)	F-score (%)	MCC (%)
1%	DAPAR	80.6 \pm 11.8	1.9 \pm 1.5	798.1 \pm 1.5	119.4 \pm 11.8	40.3 \pm 5.9	99.8 \pm 0.2	97.8 \pm 1.7	56.8 \pm 6.1	58.1 \pm 4.8
	MI4P	168.1 \pm 4.8	6.8 \pm 2.7	793.2 \pm 2.7	31.9 \pm 4.8	84 \pm 2.4	99.2 \pm 0.3	96.1 \pm 1.5	89.7 \pm 1.5	87.6 \pm 1.7
5%	DAPAR	80.9 \pm 12.6	2.4 \pm 1.8	797.6 \pm 1.8	119.1 \pm 12.6	40.4 \pm 6.3	99.7 \pm 0.2	97.2 \pm 2	56.8 \pm 6.5	58 \pm 5
	MI4P	170 \pm 4.6	7.6 \pm 2.9	792.5 \pm 2.9	30 \pm 4.6	85 \pm 2.3	99.1 \pm 0.4	95.8 \pm 1.6	90 \pm 1.4	88 \pm 1.6
10%	DAPAR	79.9 \pm 13	2.8 \pm 1.9	797.2 \pm 1.9	120.1 \pm 13	40 \pm 6.5	99.7 \pm 0.2	96.8 \pm 2	56.2 \pm 6.6	57.4 \pm 5.1
	MI4P	172.1 \pm 4.6	8.2 \pm 3	791.8 \pm 3	27.9 \pm 4.6	86.1 \pm 2.3	99 \pm 0.4	95.5 \pm 1.5	90.5 \pm 1.4	88.5 \pm 1.6
15%	DAPAR	81.8 \pm 12.9	3.6 \pm 2.5	796.4 \pm 2.5	118.2 \pm 12.9	40.9 \pm 6.4	99.6 \pm 0.3	95.9 \pm 2.5	57 \pm 6.5	57.8 \pm 5.1
	MI4P	174.2 \pm 4	9.4 \pm 3.6	790.6 \pm 3.6	25.8 \pm 4	87.1 \pm 2	98.8 \pm 0.5	94.9 \pm 1.9	90.8 \pm 1.3	88.8 \pm 1.6
20%	DAPAR	82.1 \pm 15.4	4.4 \pm 2.6	795.6 \pm 2.6	117.9 \pm 15.4	41 \pm 7.7	99.5 \pm 0.3	95.1 \pm 2.7	56.8 \pm 8	57.4 \pm 6.2
	MI4P	175.6 \pm 4.1	11.3 \pm 4.1	788.7 \pm 4.1	24.4 \pm 4.1	87.8 \pm 2.1	98.6 \pm 0.5	94 \pm 2	90.8 \pm 1.5	88.7 \pm 1.8
25%	DAPAR	83.3 \pm 14.6	5.3 \pm 2.9	794.7 \pm 2.9	116.7 \pm 14.6	41.6 \pm 7.3	99.3 \pm 0.4	94.1 \pm 2.8	57.3 \pm 7.3	57.5 \pm 5.8
	MI4P	176.3 \pm 4.5	13 \pm 3.8	787 \pm 3.8	23.7 \pm 4.5	88.1 \pm 2.3	98.4 \pm 0.5	93.2 \pm 1.9	90.6 \pm 1.5	88.4 \pm 1.8

Table S5.10: Performance evaluation on the second set of simulations imputed using principal component analysis.

%MV	Method	True positives	False positives	True negatives	False negatives	Sensitivity (%)	Specificity (%)	Precision (%)	F-score (%)	MCC (%)
1%	DAPAR	80.8 \pm 11.7	1.9 \pm 1.5	798.1 \pm 1.5	119.2 \pm 11.7	40.4 \pm 5.8	99.8 \pm 0.2	97.8 \pm 1.7	56.9 \pm 6	58.2 \pm 4.7
	MI4P	168 \pm 4.7	6.8 \pm 2.7	793.2 \pm 2.7	32 \pm 4.7	84 \pm 2.4	99.2 \pm 0.3	96.1 \pm 1.4	89.6 \pm 1.4	87.6 \pm 1.7
5%	DAPAR	80.7 \pm 12.7	2.4 \pm 1.9	797.6 \pm 1.9	119.3 \pm 12.7	40.3 \pm 6.3	99.7 \pm 0.2	97.2 \pm 2	56.7 \pm 6.5	57.9 \pm 5
	MI4P	169.9 \pm 4.4	7.5 \pm 3	792.5 \pm 3	30.1 \pm 4.4	85 \pm 2.2	99.1 \pm 0.4	95.8 \pm 1.6	90 \pm 1.4	88 \pm 1.6
10%	DAPAR	79.9 \pm 12.5	2.7 \pm 1.8	797.3 \pm 1.8	120.1 \pm 12.5	40 \pm 6.3	99.7 \pm 0.2	96.8 \pm 2	56.3 \pm 6.4	57.5 \pm 5
	MI4P	171.6 \pm 4.6	8.1 \pm 3.1	792 \pm 3.1	28.4 \pm 4.6	85.8 \pm 2.3	99 \pm 0.4	95.5 \pm 1.6	90.4 \pm 1.5	88.4 \pm 1.7
15%	DAPAR	81.4 \pm 13.8	3.5 \pm 2.4	796.5 \pm 2.4	118.6 \pm 13.8	40.7 \pm 6.9	99.6 \pm 0.3	96 \pm 2.4	56.8 \pm 7.1	57.6 \pm 5.5
	MI4P	173.5 \pm 4	9.3 \pm 3.8	790.7 \pm 3.8	26.5 \pm 4	86.8 \pm 2	98.8 \pm 0.5	94.9 \pm 1.9	90.6 \pm 1.4	88.6 \pm 1.7
20%	DAPAR	82.1 \pm 13.5	4.4 \pm 2.6	795.6 \pm 2.6	117.9 \pm 13.5	41.1 \pm 6.8	99.4 \pm 0.3	95 \pm 2.6	57 \pm 6.9	57.5 \pm 5.4
	MI4P	174.4 \pm 4.1	10.9 \pm 3.9	789.1 \pm 3.9	25.6 \pm 4.1	87.2 \pm 2	98.6 \pm 0.5	94.1 \pm 2	90.5 \pm 1.4	88.4 \pm 1.7
25%	DAPAR	82.2 \pm 16	5 \pm 2.9	795 \pm 2.9	117.8 \pm 16	41.1 \pm 8	99.4 \pm 0.4	94.4 \pm 2.8	56.8 \pm 8.5	57.2 \pm 6.7
	MI4P	174.7 \pm 4.5	12.4 \pm 4	787.6 \pm 4	25.3 \pm 4.5	87.3 \pm 2.2	98.5 \pm 0.5	93.4 \pm 1.9	90.3 \pm 1.5	88 \pm 1.8

Table S5.11: Performance evaluation on the second set of simulations imputed using random forests.

S6 Results on the third set of simulations

S6.1 Simulation design

Finally, we considered an experimental design similar to the second one, but with random effects P_i and G_{ik} . The 100 datasets were generated as follows.

1. For the first group, replicate 10 times (for the 10 variables in this group) a draw from a mixture of 2 Gaussian distributions. The first one has the following parameters: a mean of 1.5 and a standard deviation of 0.5 (corresponds to P_i). The second one has the following parameters: a mean of 0 and a standard deviation of 0.5 (corresponds to ϵ_{ij}).
2. For the second group replicate 10 times (for the 10 variables in this group) a draw from a mixture of the following 3 distributions.
 - (a) The first one is a Gaussian distribution with the following parameters: a mean of 1.5 and a standard deviation of 0.5 (corresponds to P_i).
 - (b) The second one is the mixture of a Gaussian distribution with a mean of 1.5 and a standard deviation of 0.5 for the 200 first rows (set as differentially expressed) and a zero vector for the remaining 800 rows (set as not differentially expressed). This mixture illustrates the G_{ik} term in the previous model.
 - (c) The third distribution has the following parameters: a mean of 0 and a standard deviation of 0.5 (corresponds to ϵ_{ij}).

S6.2 Performance evaluation

This subsection provides the evaluation of the `mi4p` workflow compared to the `DAPAR` workflow on the first set of simulations. The performance is described using the indicators detailed in Section S3.

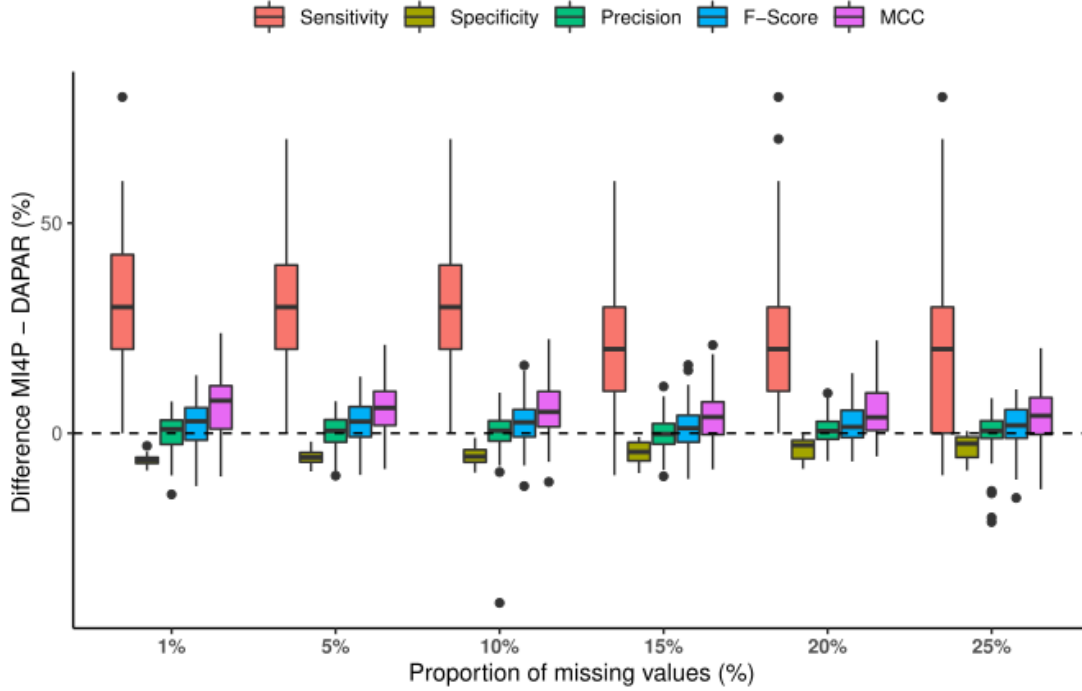


Figure S6.3: Distribution of the difference of performance between `mi4p` and `DAPAR` workflows on the third set of simulations imputed using maximum likelihood estimation.

The following tables provide results expressed as the mean of the given indicator over the 100 simulated datasets \pm the mean of the standard deviations of the given indicator over the 100 simulated datasets. Results are based on adjusted p-values using the Benjamini-Hochberg procedure [Benjamini and Hochberg, 1995] and a false discovery rate of 1%.

%MV	Method	True positives	False positives	True negatives	False negatives	Sensitivity (%)	Specificity (%)	Precision (%)	F-score (%)	MCC (%)
1%	DAPAR	25.6 \pm 10.7	0.5 \pm 0.8	799.5 \pm 0.8	174.4 \pm 10.7	12.8 \pm 5.4	99.9 \pm 0.1	98.3 \pm 2.4	22.2 \pm 8.4	31.2 \pm 7.4
	MI4P	91 \pm 10.6	2.7 \pm 1.8	797.3 \pm 1.8	109 \pm 10.6	45.5 \pm 5.3	99.7 \pm 0.2	97.2 \pm 1.8	61.8 \pm 4.9	61.9 \pm 4
5%	DAPAR	25.6 \pm 10.2	0.4 \pm 0.7	799.6 \pm 0.7	174.4 \pm 10.2	12.8 \pm 5.1	99.9 \pm 0.1	98.5 \pm 2.4	22.3 \pm 7.9	31.4 \pm 6.8
	MI4P	83 \pm 13.6	2.1 \pm 1.8	797.9 \pm 1.8	117 \pm 13.6	41.5 \pm 6.8	99.7 \pm 0.2	97.6 \pm 1.9	57.9 \pm 6.7	59 \pm 5.1
10%	DAPAR	25.9 \pm 10.8	0.6 \pm 0.7	799.4 \pm 0.7	174.1 \pm 10.8	13 \pm 5.4	99.9 \pm 0.1	96.1 \pm 14	22.5 \pm 8.6	31.1 \pm 8.3
	MI4P	80.2 \pm 18.2	2.3 \pm 2.1	797.7 \pm 2.1	119.8 \pm 18.2	40.1 \pm 9.1	99.7 \pm 0.3	97.5 \pm 2	56.2 \pm 9.2	57.6 \pm 6.9
15%	DAPAR	26.6 \pm 11.5	0.8 \pm 1	799.2 \pm 1	173.4 \pm 11.5	13.3 \pm 5.7	99.9 \pm 0.1	96.5 \pm 10.3	23 \pm 9	31.5 \pm 8.2
	MI4P	71.9 \pm 22.7	2.1 \pm 2.3	797.9 \pm 2.3	128.1 \pm 22.7	35.9 \pm 11.3	99.7 \pm 0.3	97.7 \pm 2.3	51.4 \pm 12.3	54 \pm 9.1
20%	DAPAR	28.5 \pm 12.1	1.1 \pm 1.3	798.9 \pm 1.3	171.5 \pm 12.1	14.2 \pm 6.1	99.9 \pm 0.2	95.4 \pm 10.4	24.3 \pm 9.3	32.3 \pm 8.5
	MI4P	67.1 \pm 22.4	1.9 \pm 2.3	798.1 \pm 2.3	132.9 \pm 22.4	33.6 \pm 11.2	99.8 \pm 0.3	97.8 \pm 2.3	48.8 \pm 12.4	52 \pm 9.2
25%	DAPAR	26.9 \pm 12.4	1.3 \pm 1.4	798.7 \pm 1.4	173.1 \pm 12.4	13.4 \pm 6.2	99.8 \pm 0.2	96.2 \pm 4	23 \pm 9.7	31.1 \pm 8.6
	MI4P	61.2 \pm 24	2 \pm 2.8	798 \pm 2.8	138.8 \pm 24	30.6 \pm 12	99.7 \pm 0.4	97.7 \pm 2.8	45.2 \pm 13.6	49.2 \pm 10

Table S6.12: Performance evaluation on the third set of simulation imputed using maximum likelihood estimation

%MV	Method	True positives	False positives	True negatives	False negatives	Sensitivity (%)	Specificity (%)	Precision (%)	F-score (%)	MCC (%)
1%	DAPAR	26 \pm 10.4	0.5 \pm 0.8	799.5 \pm 0.8	174 \pm 10.4	13 \pm 5.2	99.9 \pm 0.1	98.5 \pm 2.3	22.5 \pm 8.1	31.5 \pm 7
	MI4P	95.8 \pm 9.8	3.1 \pm 1.9	796.9 \pm 1.9	104.2 \pm 9.8	47.9 \pm 4.9	99.6 \pm 0.2	96.9 \pm 1.8	64 \pm 4.4	63.6 \pm 3.7
5%	DAPAR	25.4 \pm 11.1	0.4 \pm 0.7	799.6 \pm 0.7	174.6 \pm 11.1	12.7 \pm 5.5	99.9 \pm 0.1	98.5 \pm 2.5	22.1 \pm 8.7	31.1 \pm 7.5
	MI4P	98 \pm 9.9	2.9 \pm 1.8	797.1 \pm 1.8	102 \pm 9.9	49 \pm 4.9	99.6 \pm 0.2	97.1 \pm 1.7	65 \pm 4.4	64.6 \pm 3.7
10%	DAPAR	24.5 \pm 10.6	0.6 \pm 0.9	799.4 \pm 0.9	175.5 \pm 10.6	12.3 \pm 5.3	99.9 \pm 0.1	95.8 \pm 14.1	21.4 \pm 8.4	30.2 \pm 7.9
	MI4P	101.1 \pm 9.5	3.2 \pm 1.8	796.8 \pm 1.8	98.9 \pm 9.5	50.6 \pm 4.8	99.6 \pm 0.2	97 \pm 1.6	66.3 \pm 4.1	65.6 \pm 3.5
15%	DAPAR	25.1 \pm 12.2	0.4 \pm 0.7	799.6 \pm 0.7	174.9 \pm 12.2	12.5 \pm 6.1	99.9 \pm 0.1	96.4 \pm 14.1	21.7 \pm 9.7	30.4 \pm 9.2
	MI4P	103.8 \pm 10.9	2.6 \pm 1.4	797.4 \pm 1.4	96.2 \pm 10.9	51.9 \pm 5.4	99.7 \pm 0.2	97.6 \pm 1.3	67.6 \pm 4.7	66.8 \pm 4
20%	DAPAR	24.7 \pm 13.2	0.4 \pm 0.7	799.6 \pm 0.7	175.3 \pm 13.2	12.3 \pm 6.6	99.9 \pm 0.1	95.6 \pm 17.1	21.3 \pm 10.4	29.9 \pm 10.1
	MI4P	106.2 \pm 11.9	2.7 \pm 1.7	797.3 \pm 1.7	93.8 \pm 11.9	53.1 \pm 5.9	99.7 \pm 0.2	97.6 \pm 1.4	68.6 \pm 5	67.7 \pm 4.3
25%	DAPAR	24.7 \pm 12.3	0.6 \pm 0.9	799.4 \pm 0.9	175.3 \pm 12.3	12.3 \pm 6.2	99.9 \pm 0.1	96.8 \pm 10.3	21.4 \pm 9.7	30.1 \pm 8.9
	MI4P	105.4 \pm 11.1	2.9 \pm 1.9	797.1 \pm 1.9	94.6 \pm 11.1	52.7 \pm 5.5	99.6 \pm 0.2	97.4 \pm 1.6	68.2 \pm 4.7	67.3 \pm 4

Table S6.13: Performance evaluation on the third set of simulations imputed using k -nearest neighbours method.

%MV	Method	True positives	False positives	True negatives	False negatives	Sensitivity (%)	Specificity (%)	Precision (%)	F-score (%)	MCC (%)
1%	DAPAR	25.8 \pm 10.6	0.5 \pm 0.8	799.5 \pm 0.8	174.2 \pm 10.6	12.9 \pm 5.3	99.9 \pm 0.1	98.3 \pm 2.5	22.4 \pm 8.4	31.3 \pm 7.4
	MI4P	87.9 \pm 9.5	2.2 \pm 1.6	797.8 \pm 1.6	112.1 \pm 9.5	43.9 \pm 4.8	99.7 \pm 0.2	97.6 \pm 1.7	60.4 \pm 4.5	60.9 \pm 3.7
5%	DAPAR	25.6 \pm 10.7	0.5 \pm 0.7	799.5 \pm 0.7	174.4 \pm 10.7	12.8 \pm 5.4	99.9 \pm 0.1	98.4 \pm 2.4	22.3 \pm 8.4	31.3 \pm 7.3
	MI4P	63.1 \pm 10.4	0.5 \pm 0.7	799.5 \pm 0.7	136.9 \pm 10.4	31.5 \pm 5.2	99.9 \pm 0.1	99.2 \pm 1.1	47.6 \pm 6.1	51.4 \pm 4.6
10%	DAPAR	24.4 \pm 11.5	0.6 \pm 0.8	799.4 \pm 0.8	175.6 \pm 11.5	12.2 \pm 5.7	99.9 \pm 0.1	96 \pm 14.1	21.2 \pm 9.2	29.9 \pm 8.8
	MI4P	37.2 \pm 11.3	0.1 \pm 0.3	799.9 \pm 0.3	162.8 \pm 11.3	18.6 \pm 5.6	100 \pm 0	99.7 \pm 0.9	31 \pm 8.1	38.8 \pm 6.4
15%	DAPAR	24.9 \pm 12.4	0.7 \pm 0.9	799.3 \pm 0.9	175.1 \pm 12.4	12.5 \pm 6.2	99.9 \pm 0.1	95.7 \pm 14	21.6 \pm 9.7	30.1 \pm 9.2
	MI4P	17.6 \pm 11.7	0 \pm 0.2	800 \pm 0.2	182.4 \pm 11.7	8.8 \pm 5.8	100 \pm 0	92.9 \pm 25.6	15.6 \pm 9.8	24.5 \pm 11.1
20%	DAPAR	23.3 \pm 12.4	0.7 \pm 1	799.3 \pm 1	176.7 \pm 12.4	11.6 \pm 6.2	99.9 \pm 0.1	96.3 \pm 10.5	20.2 \pm 9.8	28.9 \pm 9.2
	MI4P	6.4 \pm 6.9	0 \pm 0	800 \pm 0	193.6 \pm 6.9	3.2 \pm 3.5	100 \pm 0	74 \pm 44.1	6 \pm 6.3	12.8 \pm 9.8
25%	DAPAR	24.1 \pm 11.8	0.8 \pm 1.2	799.2 \pm 1.2	175.8 \pm 11.8	12.1 \pm 5.9	99.9 \pm 0.1	97.4 \pm 3.5	21 \pm 9.3	29.7 \pm 8.2
	MI4P	1.7 \pm 3.2	0 \pm 0	800 \pm 0	198.3 \pm 3.2	0.9 \pm 1.6	100 \pm 0	43 \pm 49.8	1.7 \pm 3	5 \pm 6.8

Table S6.14: Performance evaluation on the third set of simulation imputed using Bayesian linear regression.

%MV	Method	True positives	False positives	True negatives	False negatives	Sensitivity (%)	Specificity (%)	Precision (%)	F-score (%)	MCC (%)
1%	DAPAR	25.8 \pm 10.2	0.5 \pm 0.8	799.5 \pm 0.8	174.2 \pm 10.2	12.9 \pm 5.1	99.9 \pm 0.1	98.3 \pm 2.4	22.4 \pm 8	31.4 \pm 7
	MI4P	95.7 \pm 9.9	3.2 \pm 1.8	796.8 \pm 1.8	104.3 \pm 9.9	47.9 \pm 4.9	99.6 \pm 0.2	96.8 \pm 1.7	63.9 \pm 4.4	63.5 \pm 3.7
5%	DAPAR	24.9 \pm 10.4	0.5 \pm 0.7	799.5 \pm 0.7	175.2 \pm 10.4	12.4 \pm 5.2	99.9 \pm 0.1	98.2 \pm 2.5	21.7 \pm 8.3	30.6 \pm 7.5
	MI4P	97.7 \pm 9.5	3 \pm 1.8	797 \pm 1.8	102.3 \pm 9.5	48.8 \pm 4.7	99.6 \pm 0.2	97 \pm 1.7	64.8 \pm 4.2	64.4 \pm 3.6
10%	DAPAR	24.5 \pm 10.6	0.6 \pm 0.9	799.4 \pm 0.9	175.5 \pm 10.6	12.3 \pm 5.3	99.9 \pm 0.1	95.8 \pm 14.1	21.4 \pm 8.4	30.2 \pm 7.9
	MI4P	101.1 \pm 9.5	3.2 \pm 1.8	796.8 \pm 1.8	98.9 \pm 9.5	50.6 \pm 4.8	99.6 \pm 0.2	97 \pm 1.6	66.3 \pm 4.1	65.6 \pm 3.5
15%	DAPAR	24.2 \pm 12.4	0.7 \pm 0.9	799.3 \pm 0.9	175.8 \pm 12.4	12.1 \pm 6.2	99.9 \pm 0.1	95.7 \pm 14	21 \pm 9.7	29.6 \pm 9.1
	MI4P	104.6 \pm 10.1	3.4 \pm 2.1	796.6 \pm 2.1	95.4 \pm 10.1	52.3 \pm 5.1	99.6 \pm 0.3	96.9 \pm 1.8	67.8 \pm 4.3	66.8 \pm 3.7
20%	DAPAR	23.6 \pm 12.2	0.7 \pm 0.9	799.3 \pm 0.9	176.4 \pm 12.2	11.8 \pm 6.1	99.9 \pm 0.1	94.7 \pm 17.1	20.5 \pm 9.7	29 \pm 9.7
	MI4P	110 \pm 10.1	3.7 \pm 2.1	796.3 \pm 2.1	90 \pm 10.1	55 \pm 5.1	99.5 \pm 0.3	96.8 \pm 1.7	70 \pm 4.2	68.7 \pm 3.6
25%	DAPAR	24.7 \pm 11.3	0.8 \pm 1.2	799.2 \pm 1.2	175.3 \pm 11.3	12.3 \pm 5.7	99.9 \pm 0.1	97.2 \pm 3.6	21.4 \pm 8.9	30.2 \pm 7.7
	MI4P	113.6 \pm 9.3	4.4 \pm 2.3	795.6 \pm 2.3	86.4 \pm 9.3	56.8 \pm 4.6	99.4 \pm 0.3	96.3 \pm 1.7	71.3 \pm 3.6	69.7 \pm 3.2

Table S6.15: Performance evaluation on the third set of simulation imputed using principal component analysis.

%MV	Method	True positives	False positives	True negatives	False negatives	Sensitivity (%)	Specificity (%)	Precision (%)	F-score (%)	MCC (%)
1%	DAPAR	25.7 \pm 10.2	0.5 \pm 0.7	799.5 \pm 0.7	174.3 \pm 10.2	12.8 \pm 5.1	99.9 \pm 0.1	98.5 \pm 2.3	22.3 \pm 8	31.3 \pm 7
	MI4P	95.8 \pm 9.8	3.1 \pm 1.9	796.9 \pm 1.9	104.2 \pm 9.8	47.9 \pm 4.9	99.6 \pm 0.2	96.9 \pm 1.8	63.9 \pm 4.4	63.6 \pm 3.7
5%	DAPAR	25.2 \pm 10.5	0.5 \pm 0.7	799.5 \pm 0.7	174.8 \pm 10.5	12.6 \pm 5.2	99.9 \pm 0.1	98.4 \pm 2.5	21.9 \pm 8.2	31 \pm 7.1
	MI4P	97.7 \pm 9.8	3 \pm 1.8	797 \pm 1.8	102.3 \pm 9.8	48.8 \pm 4.9	99.6 \pm 0.2	97.1 \pm 1.7	64.8 \pm 4.3	64.4 \pm 3.6
10%	DAPAR	24.4 \pm 11.4	0.5 \pm 0.8	799.5 \pm 0.8	175.6 \pm 11.4	12.2 \pm 5.7	99.9 \pm 0.1	95.2 \pm 17.1	21.2 \pm 9.1	29.9 \pm 9.1
	MI4P	102.2 \pm 9.9	2.9 \pm 1.7	797.1 \pm 1.7	97.8 \pm 9.9	51.1 \pm 4.9	99.6 \pm 0.2	97.3 \pm 1.6	66.9 \pm 4.3	66.1 \pm 3.7
15%	DAPAR	25.4 \pm 12.7	0.5 \pm 0.8	799.5 \pm 0.8	174.6 \pm 12.7	12.7 \pm 6.3	99.9 \pm 0.1	96.4 \pm 14.1	21.9 \pm 10	30.5 \pm 9.5
	MI4P	105.7 \pm 10.1	2.7 \pm 1.6	797.3 \pm 1.6	94.3 \pm 10.1	52.8 \pm 5.1	99.7 \pm 0.2	97.5 \pm 1.4	68.4 \pm 4.3	67.5 \pm 3.7
20%	DAPAR	25.1 \pm 12.5	0.4 \pm 0.7	799.5 \pm 0.7	174.9 \pm 12.5	12.5 \pm 6.3	99.9 \pm 0.1	95.6 \pm 17.1	21.7 \pm 9.8	30.4 \pm 9.5
	MI4P	110.8 \pm 10.2	3 \pm 1.9	797 \pm 1.9	89.2 \pm 10.2	55.4 \pm 5.1	99.6 \pm 0.2	97.4 \pm 1.5	70.5 \pm 4.1	69.3 \pm 3.5
25%	DAPAR	26.7 \pm 12.1	0.7 \pm 1	799.3 \pm 1	173.3 \pm 12.1	13.3 \pm 6	99.9 \pm 0.1	97.8 \pm 3.2	23 \pm 9.5	31.6 \pm 8.4
	MI4P	113.9 \pm 9.8	3.4 \pm 2	796.6 \pm 2	86.1 \pm 9.8	57 \pm 4.9	99.6 \pm 0.3	97.1 \pm 1.6	71.7 \pm 3.9	70.2 \pm 3.4

Table S6.16: Performance evaluation on the third set of simulation imputed using random forests.

S7 Real datasets generation

S7.1 Complex total cell lysates (*Saccharomyces cerevisiae* and *Arabidopsis thaliana*) spiked UPS1 standard protein mixtures

We consider a first real dataset from Muller et al. [2016]. The experiment involved six peptide mixtures, composed of a constant yeast (*Saccharomyces cerevisiae*) background, into which increasing amounts of UPS1 standard proteins mixtures (Sigma) were spiked at 0.5, 1, 2.5, 5, 10 and 25 fmol, respectively. In a second well-calibrated dataset, yeast was replaced by a more complex total lysate of *Arabidopsis thaliana* in which UPS1 was spiked in 7 different amounts, namely 0.05, 0.25, 0.5, 1.25, 2.5, 5 and 10 fmol. For each mixture, technical triplicates were constituted. The *Saccharomyces cerevisiae* dataset was acquired on a nanoLC-MS/MS coupling composed of nanoAcquity UPLC device (Waters) coupled to a Q-Exactive Plus mass spectrometer (Thermo Scientific, Bremen, Germany) as extensively described in Muller et al. [2016]. The *Arabidopsis thaliana* dataset was acquired on a nanoLC-MS/MS coupling composed of nanoAcquity UPLC device (Waters) coupled to a Q-Exactive HF-X mass spectrometer (Thermo Scientific, Bremen, Germany) as described hereafter.

S7.2 Data preprocessing

For the *Saccharomyces cerevisiae* and *Arabidopsis thaliana* datasets, Maxquant software was used to identify peptides and derive extracted ion chromatograms. Peaks were assigned with the Andromeda search engine with full trypsin specificity. The database used for the searches was concatenated in house with the *Saccharomyces cerevisiae* entries extracted from the UniProtKB-SwissProt database (16 April 2015, 7806 entries) or the *Arabidopsis thaliana* entries (09 April 2019, 15 818 entries) and those of the UPS1 proteins (48 entries). The minimum peptide length required was seven amino acids and a maximum of one missed cleavage was allowed. Default mass tolerances parameters were used. The maximum false discovery rate was 1% at peptide and protein levels with the use of a decoy strategy. For the *Arabidopsis thaliana* + UPS1 experiment, data were extracted both with and without Match Between Runs and 2 pre-filtering criteria were applied prior to statistical analysis: only peptides with at least 1 out of 3 quantified values in each condition on one hand and 2 out of 3 on the other hand were kept. Thus, 4 datasets derived from the *Arabidopsis thaliana* + UPS1 were considered. For the *Saccharomyces cerevisiae* + UPS1 experiment, the same filtering criteria were applied, but only on data extracted with Match Between Runs, leading to 2 datasets considered.

S7.3 Supplemental methods for *Arabidopsis thaliana* dataset

Peptide separation was performed on an ACQUITY UPLC BEH130 C18 column (250 mm \times 75 μ m with 1.7 μ m diameter particles) and a Symmetry C18 precolumn (20 mm \times 180 μ m with 5 μ m diameter particles; Waters). The solvent system consisted of 0.1% FA in water (solvent A) and 0.1% FA in ACN (solvent B). The samples were loaded into the enrichment column over 3 min at 5 μ L/min with 99% of solvent A and 1% of solvent B. The peptides were eluted at 400 nL/min with the following gradient of solvent B: from 3 to 20% over 63 min, 20 to 40% over 19 min, and 40 to 90% over 1 min. The MS capillary voltage was set to 2 kV at 250 °C. The system was operated in a data-dependent acquisition mode with automatic switching between MS (mass range 375–1500 m/z with R = 120 000, automatic gain control fixed at 3×10^6 ions, and a maximum injection time set at 60 ms) and MS/MS (mass range 200–2000 m/z with R = 15 000, automatic gain control fixed at 1×10^5 , and the maximal injection time set to 60 ms) modes. The twenty most abundant peptides were selected on each MS spectrum for further isolation and higher energy collision dissociation fragmentation, excluding unassigned and monocharged ions. The dynamic exclusion time was set to 40s.

S8 Results on real datasets

This section provides the evaluation of the **mi4p** workflow compared to the **DAPAR** workflow on the real datasets considered. The performance is described using the indicators detailed in Section S3. Results are based on adjusted p-values using the Benjamini-Hochberg procedure [Benjamini and Hochberg, 1995] and a false discovery rate of 1%. Missing values were imputed using maximum likelihood estimation.

S8.1 *Arabidopsis thaliana* + UPS1 experiment

Condition (vs 10fmol)	Method	True positives	False positives	True negatives	False negatives	Sensitivity (%)	Specificity (%)	Precision (%)	F-score (%)	MCC (%)
0.05fmol	DAPAR	132	3677	10507	5	96.4	74.1	3.5	6.7	15.5
	MI4P	129	2095	12089	8	94.2	85.2	5.8	10.9	21.3
0.25fmol	DAPAR	135	3466	10718	2	98.5	75.6	3.7	7.2	16.6
	MI4P	133	1974	12210	4	97.1	86.1	6.3	11.9	22.9
0.5fmol	DAPAR	134	2495	11689	3	97.8	82.4	5.1	9.7	20.2
	MI4P	132	1233	12951	5	96.4	91.3	9.7	17.6	29.1
1.25fmol	DAPAR	132	2118	12066	5	96.4	85.1	5.9	11.1	21.8
	MI4P	129	792	13392	8	94.2	94.4	14	24.4	35.1
2.5fmol	DAPAR	125	473	13711	12	91.2	96.7	20.9	34	42.8
	MI4P	93	145	14039	44	67.9	99	39.1	49.6	50.9
5fmol	DAPAR	122	1100	13084	15	89.1	92.2	10	18	28.3
	MI4P	85	383	13801	52	62	97.3	18.2	28.1	32.5

Table S8.17: Performance evaluation on the *Arabidopsis thaliana* + UPS1 dataset, filtered with at least 1 quantified value in each condition.

Condition (vs 10fmol)	Method	True positives	False positives	True negatives	False negatives	Sensitivity (%)	Specificity (%)	Precision (%)	F-score (%)	MCC (%)
5fmol	DAPAR	372	226	15522	196	65.5	98.6	62.2	63.8	62.5
	MI4P	348	179	15569	220	61.3	98.9	66	63.6	62.3

Table S8.18: Performance evaluation on the *Arabidopsis thaliana* + UPS1 dataset, filtered with at least 1 quantified value in each condition and focusing only on the comparison 5fmol vs. 10fmol.

Condition (vs 10fmol)	Method	True positives	False positives	True negatives	False negatives	Sensitivity (%)	Specificity (%)	Precision (%)	F-score (%)	MCC (%)
0.05fmol	DAPAR	74	2989	8880	3	96.1	74.8	2.4	4.7	13
	MI4P	74	2989	8880	3	96.1	74.8	2.4	4.7	13
0.25fmol	DAPAR	76	2837	9032	1	98.7	76.1	2.6	5.1	13.9
	MI4P	76	2837	9032	1	98.7	76.1	2.6	5.1	13.9
0.5fmol	DAPAR	76	1905	9964	1	98.7	83.9	3.8	7.4	17.8
	MI4P	76	1905	9964	1	98.7	83.9	3.8	7.4	17.8
1.25fmol	DAPAR	75	1411	10458	2	97.4	88.1	5	9.6	20.7
	MI4P	75	1411	10458	2	97.4	88.1	5	9.6	20.7
2.5fmol	DAPAR	70	232	11637	7	90.9	98	23.2	36.9	45.3
	MI4P	70	232	11637	7	90.9	98	23.2	36.9	45.3
5fmol	DAPAR	67	686	11183	10	87	94.2	8.9	16.1	26.7
	MI4P	67	686	11183	10	87	94.2	8.9	16.1	26.7

Table S8.19: Performance evaluation on the *Arabidopsis thaliana* + UPS1 dataset, filtered with at least 2 quantified values in each condition.

Condition (vs 10fmol)	Method	True positives	False positives	True negatives	False negatives	Sensitivity (%)	Specificity (%)	Precision (%)	F-score (%)	MCC (%)
0.05fmol	DAPAR	16	1567	6173	1	94.1	79.8	1	2	8.6
	MI4P	16	1567	6173	1	94.1	79.8	1	2	8.6
0.25fmol	DAPAR	16	1461	6279	1	94.1	81.1	1.1	2.1	9
	MI4P	16	1461	6279	1	94.1	81.1	1.1	2.1	9
0.5fmol	DAPAR	15	895	6845	2	88.2	88.4	1.6	3.2	11.1
	MI4P	15	895	6845	2	88.2	88.4	1.6	3.2	11.1
1.25fmol	DAPAR	16	880	6860	1	94.1	88.6	1.8	3.5	12.1
	MI4P	16	880	6860	1	94.1	88.6	1.8	3.5	12.1
2.5fmol	DAPAR	13	139	7601	4	76.5	98.2	8.6	15.4	25.2
	MI4P	13	139	7601	4	76.5	98.2	8.6	15.4	25.2
5fmol	DAPAR	11	419	7321	6	64.7	94.6	2.6	4.9	12.1
	MI4P	11	419	7321	6	64.7	94.6	2.6	4.9	12.1

Table S8.20: Performance evaluation on the *Arabidopsis thaliana* + UPS1 dataset, extracted without Match Between Runs and filtered with at least 1 quantified value in each condition.

Condition (vs 10fmol)	Method	True positives	False positives	True negatives	False negatives	Sensitivity (%)	Specificity (%)	Precision (%)	F-score (%)	MCC (%)
0.05fmol	DAPAR	8	1234	4119	1	88.9	76.9	0.6	1.3	6.4
	MI4P	8	1234	4119	1	88.9	76.9	0.6	1.3	6.4
0.25fmol	DAPAR	8	1150	4203	1	88.9	78.5	0.7	1.4	6.7
	MI4P	8	1150	4203	1	88.9	78.5	0.7	1.4	6.7
0.5fmol	DAPAR	8	742	4611	1	88.9	86.1	1.1	2.1	8.9
	MI4P	8	742	4611	1	88.9	86.1	1.1	2.1	8.9
1.25fmol	DAPAR	8	536	4817	1	88.9	90	1.5	2.9	10.7
	MI4P	8	536	4817	1	88.9	90	1.5	2.9	10.7
2.5fmol	DAPAR	6	83	5270	3	66.7	98.4	6.7	12.2	20.9
	MI4P	6	83	5270	3	66.7	98.4	6.7	12.2	20.9
5fmol	DAPAR	6	274	5079	3	66.7	94.9	2.1	4.2	11.3
	MI4P	6	274	5079	3	66.7	94.9	2.1	4.2	11.3

Table S8.21: Performance evaluation on the *Arabidopsis thaliana* + UPS1 dataset, extracted without Match Between Runs and filtered with at least 2 quantified values in each condition.

Condition (vs 10fmol)	Method	True positives	False positives	True negatives	False negatives	Sensitivity (%)	Specificity (%)	Precision (%)	F-score (%)	MCC (%)
0.05fmol	DAPAR	41	1040	1557	0	100	60	3.8	7.3	15.1
	MI4P	41	753	1844	0	100	71	5.2	9.8	19.1
0.25fmol	DAPAR	41	1072	1525	0	100	58.7	3.7	7.1	14.7
	MI4P	41	797	1800	0	100	69.3	4.9	9.3	18.4
0.5fmol	DAPAR	40	848	1749	1	97.6	67.3	4.5	8.6	17
	MI4P	40	585	2012	1	97.6	77.5	6.4	12	21.8
1.25fmol	DAPAR	41	409	2188	0	100	84.3	9.1	16.7	27.7
	MI4P	41	142	2455	0	100	94.5	22.4	36.6	46
2.5fmol	DAPAR	41	208	2389	0	100	92	16.5	28.3	38.9
	MI4P	40	69	2528	1	97.6	97.3	36.7	53.3	59
5fmol	DAPAR	41	475	2122	0	100	81.7	7.9	14.7	25.5
	MI4P	37	203	2394	4	90.2	92.2	15.4	26.3	35.5

Table S8.22: Performance evaluation on the *Arabidopsis thaliana* + UPS1 dataset at the protein-level, filtered with at least 1 quantified values in each condition.

S8.2 *Saccharomyces cerevisiae* + UPS1 experiment

Condition (vs 25fmol)	Method	True positives	False positives	True negatives	False negatives	Sensitivity (%)	Specificity (%)	Precision (%)	F-score (%)	MCC (%)
0.5fmol	DAPAR	188	439	18067	4	97.9	97.6	30	45.9	53.5
	MI4P	183	144	18362	9	95.3	99.2	56	70.5	72.7
1fmol	DAPAR	186	246	18260	6	96.9	98.7	43.1	59.6	64.1
	MI4P	183	71	18435	9	95.3	99.6	72	82.1	82.7
2.5fmol	DAPAR	185	161	18345	7	96.4	99.1	53.5	68.8	71.4
	MI4P	179	39	18467	13	93.2	99.8	82.1	87.3	87.4
5fmol	DAPAR	182	108	18398	10	94.8	99.4	62.8	75.5	76.9
	MI4P	156	23	18483	36	81.2	99.9	87.2	84.1	84
10fmol	DAPAR	148	109	18397	44	77.1	99.4	57.6	65.9	66.2
	MI4P	86	27	18479	106	44.8	99.9	76.1	56.4	58.1

Table S8.23: Performance evaluation on the *Saccharomyces cerevisiae* + UPS1 dataset, filtered with at least 1 quantified value in each condition.

Condition (vs 25fmol)	Method	True positives	False positives	True negatives	False negatives	Sensitivity (%)	Specificity (%)	Precision (%)	F-score (%)	MCC (%)
0.5fmol	DAPAR	131	146	16316	4	97	99.1	47.3	63.6	67.4
	MI4P	131	146	16316	4	97	99.1	47.3	63.6	67.4
1fmol	DAPAR	130	59	16403	5	96.3	99.6	68.8	80.2	81.2
	MI4P	130	59	16403	5	96.3	99.6	68.8	80.2	81.2
2.5fmol	DAPAR	130	30	16432	5	96.3	99.8	81.2	88.1	88.4
	MI4P	130	30	16432	5	96.3	99.8	81.2	88.1	88.4
5fmol	DAPAR	127	19	16443	8	94.1	99.9	87	90.4	90.4
	MI4P	127	19	16443	8	94.1	99.9	87	90.4	90.4
10fmol	DAPAR	96	18	16444	39	71.1	99.9	84.2	77.1	77.2
	MI4P	96	18	16444	39	71.1	99.9	84.2	77.1	77.2

Table S8.24: Performance evaluation on the *Saccharomyces cerevisiae* + UPS1 dataset, filtered with at least 2 quantified values in each condition.

Condition (vs 25fmol)	Method	True positives	False positives	True negatives	False negatives	Sensitivity (%)	Specificity (%)	Precision (%)	F-score (%)	MCC (%)
0.5fmol	DAPAR	42	90	2285	0	100	96.2	31.8	48.3	55.3
	MI4P	42	24	2351	0	100	99	63.6	77.8	79.4
1fmol	DAPAR	42	65	2310	0	100	97.3	39.3	56.4	61.8
	MI4P	41	13	2362	1	97.6	99.5	75.9	85.4	85.8
2.5fmol	DAPAR	41	27	2348	1	97.6	98.9	60.3	74.5	76.2
	MI4P	41	8	2367	1	97.6	99.7	83.7	90.1	90.2
5fmol	DAPAR	42	19	2356	0	100	99.2	68.9	81.6	82.6
	MI4P	41	7	2368	1	97.6	99.7	85.4	91.1	91.2
10fmol	DAPAR	39	23	2352	3	92.9	99	62.9	75	75.9
	MI4P	38	7	2368	4	90.5	99.7	84.4	87.4	87.2

Table S8.25: Performance evaluation on the *Saccharomyces cerevisiae* + UPS1 dataset, at the protein-level and filtered with at least 1 quantified values in each condition.

References

- Yoav Benjamini and Yosef Hochberg. Controlling the False Discovery Rate: A Practical and Powerful Approach to Multiple Testing. *Journal of the Royal Statistical Society. Series B (Methodological)*, 57(1):289–300, 1995. ISSN 0035-9246.
- Cheng Chang, Kaikun Xu, Chaoping Guo, Jinxia Wang, Qi Yan, Jian Zhang, Fuchu He, and Yunping Zhu. PANDA-view: An easy-to-use tool for statistical analysis and visualization of quantitative proteomics data. *Bioinformatics*, 34(20):3594–3596, October 2018. ISSN 1367-4803. doi: 10.1093/bioinformatics/bty408.
- Meena Choi, Ching-Yun Chang, Timothy Clough, Daniel Broudy, Trevor Killeen, Brendan MacLean, and Olga Vitek. MSstats: An R package for statistical analysis of quantitative mass spectrometry-based proteomic experiments. *Bioinformatics*, 30(17):2524–2526, September 2014. ISSN 1367-4803. doi: 10.1093/bioinformatics/btu305.
- Q. Gai Gianetto, S. Wiczorek, Y. Couté, and T. Burger. A peptide-level multiple imputation strategy accounting for the different natures of missing values in proteomics data. *bioRxiv*, page 2020.05.29.122770, May 2020. doi: 10.1101/2020.05.29.122770.
- Ludger J. E. Goeminne, Adriaan Sticker, Lennart Martens, Kris Gevaert, and Lieven Clement. MSqRob Takes the Missing Hurdle: Uniting Intensity- and Count-Based Proteomics. *Analytical Chemistry*, 92(9):6278–6287, May 2020. ISSN 0003-2700, 1520-6882. doi: 10.1021/acs.analchem.9b04375.
- Liang Jin, Yingtao Bi, Chenqi Hu, Jun Qu, Shichen Shen, Xue Wang, and Yu Tian. A comparative study of evaluating missing value imputation methods in label-free proteomics. *Scientific Reports*, 11(1):1760, December 2021. ISSN 2045-2322. doi: 10.1038/s41598-021-81279-4.
- Yuliya V. Karpievitch, Alan R. Dabney, and Richard D. Smith. Normalization and missing value imputation for label-free LC-MS analysis. *BMC Bioinformatics*, 13(16):S5, November 2012. ISSN 1471-2105. doi: 10.1186/1471-2105-13-S16-S5.
- Cosmin Lazar, Laurent Gatto, Myriam Ferro, Christophe Bruley, and Thomas Burger. Accounting for the Multiple Natures of Missing Values in Label-Free Quantitative Proteomics Data Sets to Compare Imputation Strategies. *Journal of Proteome Research*, 15(4):1116–1125, April 2016. ISSN 1535-3893. doi: 10.1021/acs.jproteome.5b00981.
- Qian Li, Kate Fisher, Wenjun Meng, Bin Fang, Eric Welsh, Eric B Haura, John M Koomen, Steven A Eschrich, Brooke L Fridley, and Y Ann Chen. GMSimpute: A generalized two-step Lasso approach to impute missing values

- in label-free mass spectrum analysis. *Bioinformatics*, 36(1):257–263, January 2020. ISSN 1367-4803. doi: 10.1093/bioinformatics/btz488.
- Mingyi Liu and Ashok Dongre. Proper imputation of missing values in proteomics datasets for differential expression analysis. *Briefings in Bioinformatics*, June 2020. ISSN 1477-4054. doi: 10.1093/bib/bbaa112.
- Leslie Muller, Luc Fornecker, Alain Van Dorsselaer, Sarah Cianféroni, and Christine Carapito. Benchmarking sample preparation/digestion protocols reveals tube-gel being a fast and repeatable method for quantitative proteomics. *PROTEOMICS*, 16(23):2953–2961, 2016. ISSN 1615-9861. doi: 10.1002/pmic.201600288.
- Minjie Shen, Yi-Tan Chang, Chiung-Ting Wu, Sarah J Parker, Georgia Saylor, Yizhi Wang, Guoqiang Yu, Jennifer E. Van Eyk, Robert Clarke, David M. Herrington, and Yue Wang. Comparative Assessment and Outlook on Methods for Imputing Proteomics Data. Preprint, In Review, March 2021.
- Jian Song and Changbin Yu. Missing Value Imputation using XGboost for Label-Free Mass Spectrometry-Based Proteomics Data. Preprint, Bioinformatics, April 2021.
- Stefka Tyanova, Tikira Temu, Pavel Sinitcyn, Arthur Carlson, Marco Y Hein, Tamar Geiger, Matthias Mann, and Jürgen Cox. The Perseus computational platform for comprehensive analysis of (prote)omics data. *Nature Methods*, 13(9):731–740, September 2016. ISSN 1548-7091, 1548-7105. doi: 10.1038/nmeth.3901.
- Bobbie-Jo M. Webb-Robertson, Holli K. Wiberg, Melissa M. Matzke, Joseph N. Brown, Jing Wang, Jason E. McDermott, Richard D. Smith, Karin D. Rodland, Thomas O. Metz, Joel G. Pounds, and Katrina M. Waters. Review, Evaluation, and Discussion of the Challenges of Missing Value Imputation for Mass Spectrometry-Based Label-Free Global Proteomics. *Journal of Proteome Research*, 14(5):1993–2001, May 2015. ISSN 1535-3893, 1535-3907. doi: 10.1021/pr501138h.
- Samuel Wiczorek, Florence Combes, Cosmin Lazar, Quentin Gai Gianetto, Laurent Gatto, Alexia Dorffer, Anne-Marie Hesse, Yohann Couté, Myriam Ferro, Christophe Bruley, and Thomas Burger. DAPAR & ProStaR: Software to perform statistical analyses in quantitative discovery proteomics. *Bioinformatics (Oxford, England)*, 33(1):135–136, January 2017. ISSN 1367-4811. doi: 10.1093/bioinformatics/btw580.
- Xiaoyan Yin, Daniel Levy, Christine Willinger, Aram Adourian, and Martin G. Larson. Multiple imputation and analysis for high-dimensional incomplete proteomics data. *Statistics in Medicine*, 35(8):1315–1326, 2016. ISSN 1097-0258. doi: 10.1002/sim.6800.

Wen Zhang, Yuhong Wei, Vladimir Ignatchenko, Lei Li, Shingo Sakashita, Nhu-An Pham, Paul Taylor, Ming Sound Tsao, Thomas Kislinger, and Michael F. Moran. Proteomic profiles of human lung adeno and squamous cell carcinoma using super-SILAC and label-free quantification approaches. *PROTEOMICS*, 14(6):795–803, 2014. ISSN 1615-9861. doi: 10.1002/pmic.201300382.